

**ELECTROSPINNING OF NANO HYDROXYAPATITE FILLED
POLY CAPROLACTONE / (ETHYLENE GLYCOL - ϵ -CAPROLACTONE -
ETHYLENE GLYCOL) COPOLYMER**

A DISSERTATION SUBMITTED

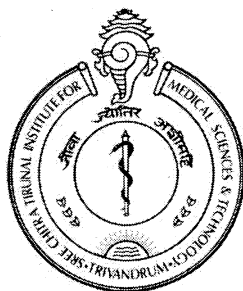
BY

RESHMI C.R.

IN PARTIAL FULFILLMENT OF THE REQUIREMENTS

FOR THE DEGREE OF

MASTER OF PHILOSOPHY



**SREE CHITRA TIRUNAL INSTITUTE FOR
MEDICAL SCIENCES AND TECHNOLOGY
TRIVANDRUM – 695 011**

DECLARATION

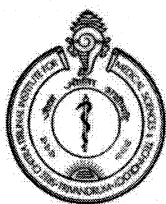
I, **Reshmi C. R.**, hereby declare that I had personally carried out the work depicted in the dissertation entitled “**Electrospinning of nano hydroxyapatite filled poly caprolactone / (ethylene glycol- ϵ -caprolactone-ethylene glycol) copolymer**” under the direct supervision of **Dr. P. Ramesh, Scientist F, Polymer Processing Laboratory** Biomedical Technology Wing, Sree Chitra Tirunal Institute for Medical Sciences and Technology, Thiruvananthapuram, Kerala, India. External help sought are acknowledged.

Signature



RESHMI C.R.

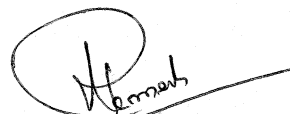
**SREE CHITRA TIRUNAL INSTITUTE
FOR MEDICAL SCIENCES & TECHNOLOGY
THIRUVANANTHAPURAM – 695011, INDIA**
*(An Institute of National Importance under Govt. of India
with the status of University by an
Act of Parliament in 1980)*



CERTIFICATE

This is to certify that the dissertation entitled “**Electrospinning of nano hydroxy apatite filled polycaprolactone/ (ethylene glycol- ϵ -caprolactone– ethylene glycol) copolymer**” submitted by **Reshmi C. R** in partial fulfilment for the Degree of Master of Philosophy in Biomedical Technology to be awarded by this Institute. The entire work was done by **her** under my supervision and guidance at **Polymer processing Lab**, Biomedical Technology Wing, Sree Chitra Tirunal Institute for Medical Sciences and Technology (SCTIMST), Thiruvananthapuram-695012.

Thiruvananthapuram


Signature

Date 30/8/2010

Name of Supervisor

The Dissertation Entitled

**ELECTROSPINNING OF NANO HYDROXYAPATITE FILLED
POLY CAPROLACTONE / (ETHYLENE GLYCOL - ϵ -CAPROLACTONE -
ETHYLENE GLYCOL) COPOLYMER**

Submitted

By

Reshmi. C. R.

For


Master of Philosophy

of

**SREE CHITRA TIRUNAL INSTITUTE FOR
MEDICAL SCIENCES AND TECHNOLOGY
TRIVANDRUM - 695 011**


Evaluated and approved

by


Signature 30/8/2010

Name of Supervisor

P. RAMESH


Signature

Examiner's name and Designation

V. KALPANA
KALPANA
S. G.

ACKNOWLEDGEMENTS

I would like to express my sincere thanks and gratitude to my guide Dr. P. Ramesh, Scientist F, Division of Polymer Processing, for his guidance and support in completing my project successfully.

I am indebted to the Director, SCTIMST and the Head, BMT wing for their generous attitude and for providing all the facilities in the completion of the course and the project. I would also like to convey my sincere thanks to the Deputy registrar for all the academic support he rendered.

My sincere thanks are due to Dr. Lissy Krishnan, Scientist G and the Course Coordinator of MPhil course for being an inspiration, rendering help whenever needed and for her great support.

I am thankful to Dr. Roy Joseph, Scientist F, for all the help offered for the completion of my project work.

I wish to express my sincere thanks to Dr. M.C. Sunny Sebastian, Scientific Officer for his ideas and help.

I wish to place on record my most sincere thanks to Ms. Remya and Mrs. Jasmin for being there for me whenever I needed help and for their patience and care.

I would like to express my heartfelt thankfulness to Mr. Arjun.G.Namboodiri, Mr. Ansar, Ms. Priya, Ms. Darsana Raghavan, Mr. Kiran, Mr. Arun and Mrs. Sreelakshmi for rendering a helpful hand in doing my project.

I am indebted to all the staff members in BCL, DPL, TIC, LPA and DTERT for their help and cooperation in doing the major part of my project work.

It is my great pleasure to thank all my batch mates, Anupriya, Jessy, Balu, Meenu, Saumi, Suja, Sreelatha, Megha, Purnima and Lekshmi, all with their cheerfulness, happiness, caring and support helped me to feel at home.

I dedicate my whole project work to my loving and caring husband Mr. Nijish Sajeevan, whose constant mental support and concern helped me to feel confident during the times of agony.

I am remembering my beloved parents, my father in law, mother in law and sweet kuku for all the support and care.

I bow my head before the Almighty God for his blessings upon me in completing the project successfully.


Reshmi C R

LIST OF ABBREVIATIONS

μm	Micrometer
DC	Direct current
DCC	Dicyclohexylcarbodiimide.
DCM	Dichloro methane
DMA	Dynamic Mechanical Analysis
DMF	N, N Dimethyl formamide
DSC	Differential scanning calorimeter
DTE-	Desaminotyrosyl-tyrosine
ECE	Ethylene glycol- ϵ -caprolactone – ethylene glycol copolymer
ECM	Extra-cellular matrix
FDA	Food and Drug Administration
FTIR	Fourier transform infra red
GPC	Gel permeation chromatography
HAP	Hydroxyapatite
HDI	Hexamethylenediisocyanate
HDPE	High density polyethylene.
Kv	Kilo volt
MTT assay	[3-(4, 5-Dimethylthiazol-2-yl)-2, 5-Diphenyltetrazolium Bromide] Assay
Nm	Nanometer
NMR	Nuclear magnetic resonance
PAA	Polyacrylic acid
PBS	Phosphate buffer saline
PCL	Polycaprolactone

PDI	Polydispersity index
PECL	Copolymers of poly (ε-caprolactone) - poly(ethylene glycol)
PEG	Poly (ethylene glycol)
PEO	Polyethylene oxide
PESu	Poly (ethylene succinate)
PHBV	Poly (hydroxybutyrate-co-valerate)
PMMA	Polymethyl methacrilate
PVA	Poly vinyl alcohol
SEM	Scanning electron microscopy
TGA	Thermogravimetric analysis
THF	Tetrahydrofuran
UTM	Universal testing machine.
μ-CT	Micro-Computed Tomography analysis

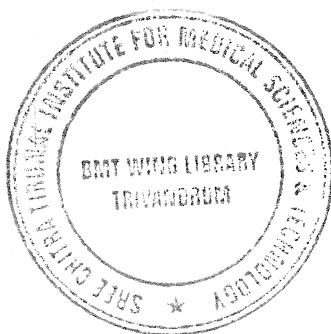


Table of Contents

Section No	Title/Sub title	Page No
	Synopsis	1
Chapter 1: Introduction		
1.1	Background	4
1.2	Literature review	6
1.2.1	Biomaterials	6
1.2.2	Electrospinning	9
1.2.2.1	Parameter Investigation	11
	• Applied voltage	11
	• Flow rate	12
	• Solution parameters	13
	• Polymer concentration	13
	• Conductivity/solution charge density	13
	• Surface tension	14
	• Polymer molecular weight	14
	• Solvent volatility	15
	• Capillary -collector distance	15
	• Needle tip design and placement	16
	• Collector composition and geometry	16
	• Ambient parameters	17
1.2.2.2	Applications of Nanofibers	18
	• Medical prostheses	18

	• Wound dressing	18
	• Drug delivery and pharmaceutical composition	19
	• Bone tissue engineering	19
1.2.3	Polycaprolacton	20
1.2.4	Hydroxyapatite (HA)	23
1.2.5	Polyethylene Glycol	25
1.2.6	Copolymers	26
1.3	Gap	28
1.4	Hypothesis	29
1.5	Objective	30
Chapter 2: Materials and methods		31
2.1.	Synthesis of PEG-PCL-PEG (ECE) triblock co polymer	31
2.1.1	Materials	31
2.1.2	Method	31
2.2	Characterization of the PEG-PCL-PEG (ECE) triblock co polymer	33
2.2.1	Chemical Characterization	33
2.2.1.1	Fourier transformation infrared spectroscopy (FTIR)	33
2.2.1.2	Nuclear magnetic resonance analysis (¹ H-NMR)	33
2.2.2	Physical Characterization	34
2.2.2.1	Gel permeation chromatography analysis (GPC)	34
2.2.3	Thermal Characterization	34
2.2.3.1	Thermogravimetric analysis (TGA)	34
2.2.3.2	Differential scanning calorimetry	35
2.3	Characterization of Hydroxyapatite	36
2.3.1	Particle size analysis	36
2.4	Fabrication of scaffold	37
2.4.1	Preparation of Spinning dopes	37

2.4.2	Electrospinning process	38
2.4.3	Characterization of scaffolds	39
2.4.3.1	Morphological observation using Scanning Electron Microscopy (SEM)	39
2.4.3.2	Mechanical Characterization using UTM & DMA	40
	✦ Universal Testing Machine(UTM)	40
	✦ Dynamic Mechanical Analysis (DMA)	41
2.4.3.3	Porosity measurement using Micro-Computed Tomography analysis (μ -CT)	42
2.4.3.4	In-Vitro degradation tests in phosphate buffer saline (PBS)	42
2.4.3.5	Cytotoxicity evaluation using MTT assay	43
Chapter 3: Results and Discussion		44
3.1	Fourier Transformation Infrared Analysis (FTIR) of NCO Terminated PCL Prepolymer and the triblock copolymer ECE	44
3.2	Nuclear Magnetic Resonance Spectroscopy of ECE copolymer	46
3.3	Gel Permeation Chromatography analysis of ECE copolymer	47
3.4	Thermogravimetric analysis (TGA) of ECE copolymer	48
3.5	Differential Scanning Calorimetric (DSC) analysis of copolymer ECE	49
3.6	Characterization of Hydroxyapatite (HAP) using Particle size analyzer	50
3.7	Fabrication & Characterization of Scaffolds	50
3.7.1	Effect of PCL concentration	51
3.7.2	Effect of filler content	55
3.7.3	Effect of triblock copolymer ECE	58
3.7.4	Effect of Applied Potential	60
3.7.5	Effect of Flow Rate	62
3.7.6	Effect of Solvent ratio	63
3.8	Comparison of PCL, PCL/HAP, PCL/ECE and PCL/ECE/HAP	65

3.8.1	Morphological characterization	66
3.8.2	Mechanical Characterization of scaffolds	67
3.8.2.1	Universal Testing Machine (UTM)	67
3.8.2.2	Dynamic Mechanical Analysis (DMA)	69
3.8.3	Porosity of Scaffolds	70
3.8.4	In-vitro degradation studies of scaffolds in PBS	73
3.8.5	Cytotoxicity evaluation of scaffolds using MTT assay	75
Chapter 4: Summary & Conclusion		77
Future scope		78
Appendix		79
Reference		80

3.8.1	Morphological characterization	66
3.8.2	Mechanical Characterization of scaffolds	67
3.8.2.1	Universal Testing Machine (UTM)	67
3.8.2.2	Dynamic Mechanical Analysis (DMA)	69
3.8.3	Porosity of Scaffolds	70
3.8.4	In-vitro degradation studies of scaffolds in PBS	73
3.8.5	Cytotoxicity evaluation of scaffolds using MTT assay	75
Chapter 4: Summary & Conclusion		77
Future scope		78
Appendix		79
Reference		80

List of Figures

Fig No	Caption	Page No
1.1	Electrospin setup	10
1.2	Electrospinning set up with rotating mandrel as collector	17
1.3	Conversion of caprolactone to polycaprolactone	21
1.4	Nano hydroxyapatite cluster	24
1.5	Polyethylene Glycol	26
2.1	Functionalization of telechelic PCL diol with HDI	31
2.2	Synthesis of ECE triblock copolymer	32
2.3	Electrospinning apparatus	38
2.4	Universal Testing Machine	40
2.5	DMA	41
3.1	FTIR spectrum of the NCO terminated PCL prepolymer	45
3.2	FTIR spectra of copolymer ECE	46
3.3	^1H NMR spectra of the PEG-PCL-PEG triblock copolymer	47
3.4	GPC analysis of ECE	48
3.5	TGA of copolymer ECE	49
3.6	DSC of copolymer ECE	49
3.7	Particle size distribution of HAP	50
3.8	SEM micrographs of the electrospun PCL samples at different concentrations; (a) 8% (b) 10% (c) 12% (d) 15% and (e) 20%	53
3.9	Effect of filler content on mechanical strength	56
3.10.	SEM micrographs of the electrospun PCL samples at different HAP concentrations; (a) 0.5 wt%, (b) 1 wt%, (c) 2 wt%, (d) 4 wt % and (e) 6 wt%	58
3.11	SEM micrographs of the electrospun PCL/ECE at different copolymer ratio (a) 90:10 (b) 80:20 (c) 70:30)	59

List of Figures

Fig No	Caption	Page No
1.1	Electrospin setup	10
1.2	Electrospinning set up with rotating mandrel as collector	17
1.3	Conversion of caprolactone to polycaprolactone	21
1.4	Nano hydroxyapatite cluster	24
1.5	Polyethylene Glycol	26
2.1	Functionalization of telechelic PCL diol with HDI	31
2.2	Synthesis of ECE triblock copolymer	32
2.3	Electrospinning apparatus	38
2.4	Universal Testing Machine	40
2.5	DMA	41
3.1	FTIR spectrum of the NCO terminated PCL prepolymer	45
3.2	FTIR spectra of copolymer ECE	46
3.3	^1H NMR spectra of the PEG-PCL-PEG triblock copolymer	47
3.4	GPC analysis of ECE	48
3.5	TGA of copolymer ECE	49
3.6	DSC of copolymer ECE	49
3.7	Particle size distribution of HAP	50
3.8	SEM micrographs of the electrospun PCL samples at different concentrations; (a) 8% (b) 10% (c) 12% (d) 15% and (e) 20%	53
3.9	Effect of filler content on mechanical strength	56
3.10.	SEM micrographs of the electrospun PCL samples at different HAP concentrations; (a) 0.5 wt%, (b) 1 wt%, (c) 2 wt%, (d) 4 wt % and (e) 6 wt%	58
3.11	SEM micrographs of the electrospun PCL/ECE at different copolymer ratio (a) 90:10 (b) 80:20 (c) 70:30)	59

3.12	SEM micrographs of the electrospun PCL/ECE/HAP samples at different Applied potentials; (a) 12kv, (b) 15kv, (c) 17kv, and (d) 20kv.	61
3.13	SEM micrographs of the electrospun PCL/ECE/HAP samples at different flow rates: (a) 0.5 ml/hr, (b) 1ml/hr, (c) 2ml/hr, (d) 3ml/hr.	63
3.14	SEM micrographs of the electrospun PCL/ECE/HAP samples at different solvent ratios: DCM/DMF (a) 90:10, (b) 80:20, (c) 70:30, (d) 60:40. (E) 50:50	65
3.15	SEM emages of (a)PCL,(b) PCL/HAP,(c)PCL/ECE,(d)PCL/ECE/HAP electrospun samples	67
3 16	Mechanical properties of PCL, PCL/HAP, PCL/ECE, PCL/ECE/HAP electrospun samples	68
3.17	Storage modulus of scaffolds as a function of temperature	69
3.18	Tan delta of scaffolds as a function of temperature	70
3.19	Comparative study on the average pore size and % porosity of Scaffolds	71
3.20	Pore size distribution curves of (a)PCL,(b)PCL/HAP,(c)PCL/ECE,(d)PCL/ECE/HAP scaffolds	72
3.21	Micro-CT 3D morphology images of electrospun scaffolds (a)PCL,(b)PCL/HAP,(c)PCL/ECE,(d)PCL/ECE/HAP	73
3.22	Degradation in Tensile Strength of Electrospun samples	74
3.23	SEM images after 28 days aging in PBS (a)PCL,(b)PCL/HAP.(c)PCL/ECE(d)PCL/ECE/HAP	75
3.24	MTT assay of the four PCL,PCL/HAP,PCL/ECE,PCL/ECE/HAP scaffolds	76

List of Tables

Table No	Caption	Page No
1.1	Applications of Synthetic Materials and Modified Natural Materials in Medicine	7
3.1	Effect of solution concentration on fiber diameter and tensile strength	54
3.2	Effect of filler content on fiber diameter and tensile strength	56
3.3	Effect of copolymer concentration in fiber diameter and tensile strength	59
3.4	Effect of applied voltage on fiber diameter	60
3.5	Effect of flow rate on fiber diameter	62
3.6	Effect of solvent ratios on fiber diameter	64
3.7	Fiber diameter of PCL,PCL/HAP,PCL/ECE,PCL/ECE/HAP scaffolds	66
3.8	Mechanical properties of scaffolds using UTM	68

Synopsis

Injuries and diseases related to the musculoskeletal system plague millions of individuals each year. While autograft procedures, where bone is removed from another area of the patient's skeleton and implanted into the defect, are considered by many orthopedic surgeons to be the best option for treating large bone defects, these procedures still have many limitations. For instance, bone grafting requires a second surgical site, is limited in quantity, and is restricted regarding the integration of implanted bone and vascular structures with native tissue. As an alternative approach, bone tissue engineering offers a promising new approach to repair of bone fractures with bone loss, fractures that do not heal, and fractures due to bone tumors. Bone tissue engineering is an emerging area where new opportunities are possible by the use of nanostructured biomaterials, which could replace hard and soft skeletal tissue. Electrospinning or electrostatic spinning has emerged as a very popular technique to fabricate polymeric nanofibrous structures for tissue engineering. Electrospun nanofiber matrices in various forms including thick nanofiber sheets, tubular structures, and as a coating material have been used in a variety of biomedical applications.

A number of biodegradable and bioresorbable materials, as well as scaffold designs, have been experimentally and/or clinically studied. Polycaprolactone (PCL) is a biodegradable synthetic polymer that is currently used in a number of biomedical applications. However, poor mechanical properties, intrinsic hydrophobic nature and slower resorption kinetics of PCL impair its use as material scaffold for hard tissue replacement. Therefore strategies to improve mechanical performance, hydrophilicity and degradation profile of PCL based scaffolds are needed. Copolymers consisting of hydrophobic polycaprolactone blocks and hydrophilic polyethyleneglycol block have attracted the interest of material scientists in this regard but polyethylene glycols are incompatible with polycaprolactone owing to their large difference in hydrophilic and hydrophobic nature.

The present study aims at synthesizing a triblock copolymer of the type PEG-PCL-PEG by coupling reaction between polyethylene glycol and polycaprolactone and further blending this copolymer with PCL to improve the hydrophilicity and biodegradation rate of PCL. Pristine and composite scaffolds using PCL and PCL/ECE blends were fabricated by electrospinning process by adopting nano hydroxyapatite as the reinforcement. A comparative study of physico-mechanical properties, biostability and cytotoxicity with L929 cells were conducted for PCL, PCL/ECE, PCL/HAP and PCL/ECE/HAP scaffolds. The results of each stage were very promising, the reaction yield for the synthesis of copolymer was around 72% and the chemical composition and structural elucidation were done by utilizing FTIR, ^1H NMR, GPC and TGA. The structural analysis using FTIR and NMR supports the formation of copolymer. The GPC analysis showed a monomodal molecular weight distribution with polydispersity index of 1.038. The thermo gravimetric analysis indicated that the copolymer is thermally stable up to 201°C. The influence of solution concentration on the morphology of electrospun fibers was initially investigated for PCL. As revealed by SEM images, fibers exhibited a rougher surface morphology with increasing solution concentration. The effect of synthesized copolymer and the filler HAP on mechanical and morphological property of PCL was also evaluated. Mechanical properties depict a non homogenous distribution of HAP particles at loadings beyond 2 wt%. Based on the observations, an optimum solution concentration of 10%, HAP content of 2 wt% and PCL to ECE ratio of 90:10 was chosen. The effect of processing parameters such as applied potential and feed rate on the morphology of the hydroxyapatite filled PCL/ECE blends was investigated. A reduction in fiber diameter was observed with increasing potential (up to 17kV) whereas the fiber diameter increased with increasing feed rate. Minimum fiber diameter was observed with feed rate of 1mL/h. It was also observed that minimum fiber diameter was observed with feed rate 1mL/h and 50:50 solvent ratio (DCM & DMF). Micro computed tomography analysis revealed a reduction in scaffold porosity from 92 to 80% with the incorporation of nano HAP. The addition of ECE to neat PCL significantly reduced the

porosity to about 74%. Hence it is clear that the incorporation of both ECE and HAP caused an overall decrease in porosity. *In vitro* biodegradation negatively impacted the mechanical properties of all the four scaffolds. The cytocompatibility evaluation was conducted with mouse fibroblasts cells and all the scaffolds showed non cytotoxic response. The results are quite promising and this new composite scaffold can act as a bespoke material for bone tissue engineering.

Chapter 1

INTRODUCTION

1.1 Background

A paradigm shift is taking place in medicine from using synthetic implants and tissue grafts to a tissue engineering approach that uses degradable porous scaffolds. Materials for making scaffold matrices include biomaterials such as natural /synthetic polymers, ceramics and composites. Many polycaprolactone (PCL) based devices such as drug delivery devices, sutures and cranioplasty implants have been approved by Food and Drug Administration (FDA) for use in the human body. PCL is degraded by hydrolysis of its ester linkages in physiological conditions and has therefore received a great deal of attention for use as an implantable biomaterial. In particular it is especially interesting for the preparation of long term implantable devices, owing to its slower degradation. It is being investigated as a scaffold for tissue repair via engineering. The poor mechanical properties of PCL, depending on the preparation technique and molecular weight, impair its use as a material scaffold for hard tissue replacement. Also PCL has an intrinsic hydrophobic chemical nature with poor surface wetting and interaction in biological fluids. The above drawback may obstruct its biomedical applications.

Considering the potentials of PCL, it is possible to design a scaffold with desired properties by appropriate modifications. A number of novel approaches have been developed for the fabrication of biomaterial-based three-dimensional scaffolds. The electrospinning technique which has been actively explored recently; can architecturally fabricate and mimic the chemical, physical and mechanical properties of the native extracellular matrix (ECM). Polymeric nanofiber woven/non woven matrix is among the most promising biomaterials for native ECM analogs. In fact, microscaled polymeric

nonwoven mesh has already been widely used in tissue engineering because of its high surface area and high porosity. The simplicity with which nanofibrous polymeric scaffolds are produced by electrospinning has invigorated interest in many biomedical applications, such as tissue engineering, wound dressing, enzyme immobilization and drug delivery. For a specific successful application, the chemical, physical and biological properties of electrospun scaffolds should be adjusted to match the environment by using a combination of multi-component compositions. Physical and biological properties, such as hydrophilicity, mechanical modulus and strength, biodegradability, biocompatibility, and specific cell interactions, are largely dependent on the chemical compositions of polymer electrospun scaffolds. Polymer blending and copolymerization are two effective means to combine different polymers to yield new materials properties. Designing composites scaffolds utilizing osteogenic and osteoinductive inorganic phases such as hydroxyapatite confers its high bioactivity as well as mechanical stability to the polymer matrix. Thus, by selecting a combination of proper components and by adjusting the component ratio, properties of electrospun scaffolds can be tailored with desired new functions.

Though the electrospinning technique has several advantages, it is critical to understand and optimize several issues such as consistency of processing method, optimization of structure and properties of scaffold including pore size, porosity, mechanical property, biostability and cytocompatibility.

1.2 Literature Review

1.2.1 Biomaterials

Biomaterial is any material, natural or man-made, that comprises whole or part of a living structure or biomedical device which performs, augments, or replaces a natural function. Although biomaterials are primarily used for medical applications, they are also used to grow cells in culture, in apparatus for handling proteins in the laboratory, in devices to regulate fertility in cattle, in the aquaculture of oysters, and possibly in the near future they will be used in a cell-silicon "biochip" that would be integrated into computers. The common thread is the interaction between biological systems and synthetic (or modified natural) materials. A biomaterial must always be considered in the context of its final fabricated, sterilized form.

Many definitions have been proposed for the term "biomaterial." One definition, endorsed by a consensus of experts in the field, is: "A biomaterial is a nonviable material used in a medical device, intended to interact with biological systems." [Williams, 1987]. In 2009 Williams redefined the definition of biomaterial as "A biomaterial is a substance that has been engineered to take a form which, alone or as part of a complex system, is used to direct, by control of interactions with components of living systems, the course of any therapeutic or diagnostic procedure, in human or veterinary medicine." A complementary definition essential for understanding the goal of biomaterials science, is that of "biocompatibility." "Biocompatibility is the ability of a material to perform with an appropriate host response in a specific application. [Williams, 1987]. Biocompatibility is related to the behavior of biomaterials in various environments under various chemical and physical conditions.

A biomaterial should be non toxic and biocompatible one. For example, polymers, many low-molecular-weight "leachables" exhibit some level of physiologic

activity and cell toxicity. It is reasonable to say that a biomaterial should not give off anything from its mass unless it is specifically designed to do so. [Ratner *et.al.*, 1996]

Table 1.1 Applications of Synthetic Materials and Modified Natural Materials in Medicine

Application	Types of materials
Skeletal system	
Joint replacements (hip, knee)	Titanium, Ti—Al—V alloy, Stainless steel, polyethylene
Bone plate for fracture fixation	Stainless steel, cobalt—chromium alloy
Bone cement	Poly (methyl methacrylate)
Bony defect repair	Hydroxylapatite
Artificial tendon and ligament	Teflon, Dacron
Dental implant for tooth fixation	Titanium, alumina, calcium Phosphate
Cardiovascular system	
Blood vessel prosthesis	Dacron, Teflon, polyurethane
Heart valve	Reprocessed tissue, stainless steel, carbon
Catheter	Silicone rubber, Teflon, polyurethane
Organs	
Artificial heart	Polyurethane

Skin repair template	Silicone-collagen composite
Artificial kidney (hemodialyzer)	Cellulose, polyacrylonitrile
Heart—Lung machine	Silicone rubber
Senses	
Cochlear replacement	Platinum electrodes
Intraocular lens	Poly (methyl methacrylate), silicone rubber, hydrogel
Contact lens	Silicone—acrylate, hydrogel
Corneal bandage	Collagen, hydrogel

Biomaterial scaffolds are used for tissue engineering application. Tissue engineering has been recognized as an alternative technique to whole-organ and tissue transplantation for diseased, failed, or malfunctioned organs. It is an emerging area of applied research with a goal of repairing or regenerating the functions of damaged tissue that fails to heal spontaneously by using cells and synthetic functional components called scaffolds.[Murugan & Ramakrishna.,2007]

A scaffold provides a 3-D framework for the cells to attach and develop in vitro [Liu *et al.*1996]. It acts as a temporary support for the cells to adhere and proliferate. An ideal tissue-engineered scaffold should be mechanically stable and capable of functioning biologically in the implant site. Mechanical stability is dependent primarily on the selection of the biomaterial, the architectural design of the scaffold, and the cell material interactions. It should mimic native ECM both architecturally and functionally. A tissue engineering scaffold should be biodegradable so that a second surgery is not required to

remove the implant. The rate of degradation should coincide or at least be controllable to mimic the rate of neo-tissue formation. [Hutmacher., 2000].

Many techniques are employed for scaffold fabrication in tissue engineering. Fibrous scaffolds are attractive for tissue engineering because of their inherent advantages of high surface area for cell attachment, controlled porous architecture, and a 3-D microenvironment for cell-cell contact. Nanofibers composed of natural or synthetic biodegradable polymers can be tailor-designed to possess the tissue matching mechanical compliance. The orientation of these fibers is considered as one of the important features of a perfect tissue scaffold, because the fiber orientation greatly influences cell growth and related functions. Therefore, engineering scaffolds with a control over fiber orientation is essential and a prerequisite for controlling cell orientation and tissue growth. Electrospinning is a straightforward, cost-effective, and versatile method, which is recently applied in engineering well-defined nano-fibrous scaffolds that hold promise in serving as a synthetic extra-cellular matrix (ECM). This technology enables to architecturally fabricate and mimic the chemical, physical and mechanical properties of the native extra-cellular matrix (ECM). [Chew *et al.*, 2006]

1.2.2 Electrospinning

Electrospinning has vast applications due to an increased interest in nanoscale properties and technologies. This technique allows for the production of polymer fibers with diameter varying from 3 nm to 5 μm . Potential applications of electrospinning include filtration membrane, catalytic nanofibers, fiber based sensors, and tissue engineering scaffolds [Pham *et al.*, 2006].

One attractive feature of electrospinning is the simplicity and inexpensive nature. The electrospin setup consist of a capillary through which the liquid is to be electrospun is forced: high voltage source with negative and positive polarity, which injects the

charge into the liquid: and a grounded collector set up. (fig 1.1) [Sill and Von Recum., 2008]

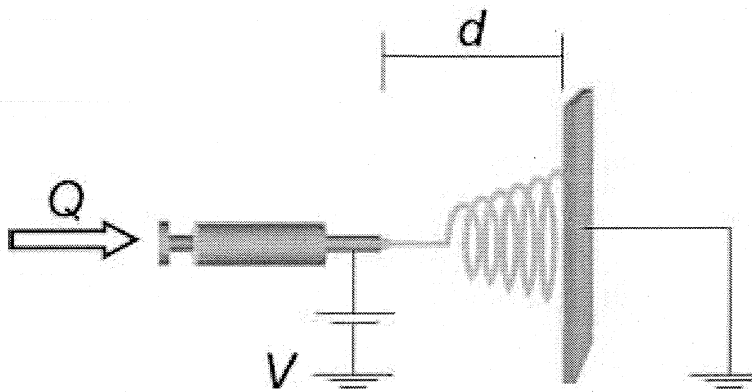


Fig 1.1 Electrospin setup

Although the term “electro spinning”, derived from ‘electrostatic spinning’. The polymer filaments were formed, from the solution, between two electrodes bearing electrical charges of opposite polarity. One of the electrodes was placed into the solution and the other onto a collector. Once ejected out of a metal spinneret with a small hole, the charged solution jets evaporated to become fibers which were collected on the collector. The potential difference depended on the properties of the spinning solution, such as polymer molecular weight and viscosity.

So far, we have found in the open literature that more than fifty different polymers have been successfully electrospun into ultra fine fibers with diameters ranging from <3 nm to over $1 \mu\text{m}$. Most of the polymers were dissolved in some solvents before electrospinning. When the solid polymer or polymer pellet is completely dissolved in a proper amount it becomes a fluid form called polymer solution. The polymer fluid is then introduced into the capillary tube for electrospinning, a DC of very high KVs is necessary to generate the electrospinning.

Electrospun fibers have high porosity similar to the natural extracellular matrix (ECM). Electrospun fibers can be oriented or arranged randomly, giving control over both the bulk mechanical properties and the biological response to the scaffold. The diameters of polymer fiber materials are shrunk from micrometers (e.g. 10–100 μm) to sub microns or nanometers, there appear several amazing characteristics such as very large surface area to volume ratio (this ratio for a nano fiber can be as large as 103 times of that of a micro fiber), flexibility in surface functionalities, and superior mechanical performance (e.g. stiffness and tensile strength) compared with any other known form of the material. [Ming Huang *et al.*, 2006].

1.2.2.1 Parameter Investigation

Many parameters can influence the transformation of polymer solutions into nanofibers through electrospinning. These parameters are applied voltage, flow rate, the solvent parameters such as polymer concentration (viscosity), elasticity, conductivity, and surface tension solvent volatility and variables such as the gap (distance between the tip and the collecting screen), ambient parameters such as solution temperature, humidity, and air velocity in the electrospinning chamber, Needle tip design and placement.

- **Applied voltage**

The strength of the applied electric field controls formation of fibers from several microns in diameter to tens of nanometers. Sub optimal field strength could lead to bead defects in the spun fibers or even failure in jet formation. Deitzel *et al.* examined a polyethylene oxide (PEO)/water system and found that increases in applied voltage altered the shape of the electrospun fibers. At low voltages or field strengths, a drop is typically suspended at the needle tip, and a jet will originate from the Taylor cone producing bead-free spinning when the force of the electric field is sufficient to overcome the surface tension [Deitzel *et al.*, 2001]. As the voltage is increased, the volume of the drop at the tip decreases, causing the Taylor cone to recede. As the voltage is increased

further, the jet eventually moves around the edge of the tip, with no visible Taylor cone; at these conditions, the presence of many beads can be observed [Zong *et al.*, 2002]. So there is a voltage limit in which the smooth fine fibers will obtain.

Meechaisue *et al* examined the effect of varying the applied electric field strength from 10 to 25 kV/10 cm for poly (DTE carbonate) solutions with polymer concentrations of 15 and 20% (w/v). For the 15% (w/v) poly(DTE carbonate) solution the author observed primarily beaded fibers when the applied electric field strength was below 20 kV/10 cm, while mostly smooth fibers were obtained above this field strength. Increasing the electric field strength from 10 to 15 kV/10 cm decreased the bead density, while increasing the field strength from 20 to 25 kV/10 cm increased the average fiber diameter from 1.9 to 2.2 μm . The authors attribute the increase in fiber diameter to the increase in the mass flow rate relative to the increase in the electrostatic force. For the 20% (w/v) poly(DTE carbonate) solution only smooth fibers were obtained at all electric field strengths. Additionally, the average fiber diameter was found to increase monotonically from about 2.5 μm at 10 kV/10 cm to about 5.4 μm at 25 kV/10 cm, while the fiber density monotonically decreased over this same range. Based on the work by Deitzel *et al.*, Meechaisue *et al.* and others it is evident that there is an optimal range of electric field strengths for a certain polymer/solvent system, as either too weak or too strong field will lead to the formation of beaded fibers.

- **Flow rate**

Polymer flow rate also has an impact on fiber size, and influence fiber porosity as well as fiber shape. Megelski *et al.* examined the effects of flow rate on the structure of electrospun fibers from a polystyrene/tetrahydrofuran (THF) solution [Megelski *et al.*, 2002]. They demonstrated that both fiber diameter and pore size increase with increasing flow rate. Additionally, at high flow rates significant amounts of bead defects were noticeable, due to the inability of fibers to dry completely before reaching the collector.

Incomplete fiber drying also leads to the formation of ribbon like (or flattened) fibers as compared to fibers with a circular cross section.

Solution Parameters

- **Polymer concentration**

Polymer concentration is an important parameter which affects the morphology of electrospun fibers. Fong et al. recognized that higher polymer concentration resulted in fewer beads. The shape of the beads changed from spherical to spindle like when the polymer concentration varied from low to high levels. Reducing surface tension of a polymer solution, fibers could be obtained without beads [Fong *et al.*, 1999].

One of the most important quantities related with electrospinning is the fiber diameter. The fiber diameters will depend primarily on the jet sizes as well as on the polymer contents in the jets. The polymer concentration influences both viscosity and the surface tension, both of them are very important parameters for electrospinning. Most significant parameters influencing the fiber diameter is the solution viscosity. The fibers from low viscosity solutions tended to be shorter and finer whereas those from more viscous solutions were relatively continuous [Baumgarten *et al.*, 1971, Doshi and Reneker., 1995, Fong *et al.*, 1999]. However, when a solid polymer is dissolved in a solvent, the solution viscosity is proportional to the polymer concentration. Thus, the higher the polymer concentration the larger the resulting nanofiber diameters will be. In fact, Deitzel *et al.* pointed out that the fiber diameter increased with increasing polymer concentration according to a power law relationship [Deitzel *et al.* 2001]. Demir *et al.* further found that the fiber diameter was proportional to the cube of the polymer concentration [Demir *et al.* 2002].

- **Conductivity / solution charge density**

Increasing the solution conductivity or charge density can be used to produce more uniform fibers with fewer beads [Jiang *et al.*, 2004]. One approach to increasing

solution conductivity has been through the addition of salt; beading decreased upon the addition of salt. Conductivity has been increased by the addition of alcohol to the solvent, resulting in smoother fibers of poly (hydroxybutyrate-co-valerate) (PHBV) with fewer beads present. Addition of tetrachloromethane, which reduced the solution conductivity, produced larger beads [Zuo *et al.*,2005]. Zhang *et al.* showed that PVA fiber diameters were decreased from 214 ± 19 nm to 159 ± 21 nm when NaCl concentration was increased from 0.05 to 0.2% (spinning conditions: solvent - water, voltage - 5 kV, distance to collector - 10 cm, flow rate - 0.2 mL/h). Zong *et al.* studied the effect of the addition of various salts (NaCl, KH_2PO_4 , NaH_2PO_4) to PDLA solutions. They found that salts with smaller ionic radii produced smaller fibers (210 nm) while salts with larger ionic radii yielded larger ones (1000 nm).They attributed this difference to the higher charge density, and thereby mobility, of ions with smaller radii; the higher mobility resulted in increased elongational forces exerted on the fiber jet yielding a smaller fiber [Zong *et al.*,2002].

- **Surface tension**

The impact of surface tension on the morphology and size of electrospun fibers has also been investigated. An increase in surface tension increases the beading. The addition of ethanol to PEO and PVA solutions lowered the surface tension. In the case of the PEO, the solution containing ethanol exhibited less beading; [Fong et al 1999] however, when ethanol was added to PVA solutions, beading was increased. The difference in the effect of adding ethanol to these systems was attributed to the fact that it is a non-solvent for PVA and a solvent for PEO [Lee *et al.*, 2004].

- **Polymer molecular weight**

Researches have examined the relationship between polymer molecular weight and the morphology and size of electrospun fibers. Gupta *et al* found as the molecular weight increased, the number of beads and droplets was reduced. Additionally, PMMA

with a narrow molecular weight distribution gave uniform fibers at a lower concentration than those with larger molecular weight distributions [Gupta *et al.*, 2005].

- **Solvent volatility**

Choice of solvent is also critical parameter. In order to have sufficient solvent evaporation to occur between the capillary tip and the collector a volatile solvent must be used. As the fiber jet travels through the atmosphere toward the collector a phase separation occurs before the solid polymer fibers are deposited, a process that is greatly influenced by the volatility of the solvent. Megelski *et al.* examined the structural properties of polystyrene fibers electrospun from solutions containing various ratios of DMF and THF [Megelski *et al.*, 2002]. Solutions electrospun from 100% THF (more volatile) demonstrated a high density of pores, which increased the surface area of the fiber by as much as 20-40% depending on the fiber diameter. Solutions electrospun from 100% DMF (less volatile) demonstrated almost a complete loss of micro texture with the formation of smooth fibers. Between these two extremes it was observed that pore size increased with decreased pore depth (thus decreasing pore density) as the solvent volatility decreased. As mentioned previously a phase separation occurs as the polymer jet is traveling through the atmosphere, this phase separation can be vapor-induced, non-solvent from the vapor phase penetrates to the polymer solution [Deitzel *et al.*, 2001].

- **Capillary -collector distance**

The distance between capillary tip and collector can also influence fiber size. Additionally, this distance can dictate whether the end result is electrospinning or electrospraying. Doshi and Reneker found that the fiber diameter decreased with increasing distances from the Taylor cone [Doshi *et al.*, 1995]. In another study, Jaeger *et al.* electrospun fibers from a PEO/water solution and examined the fiber diameter as a function of the distance from the Taylor cone [Jaeger *et al.*, 1998]. They found that the

diameter of the fiber jet decreased approximately two-fold, from 19 to 9 μm after traveling distances of 1 and 3.5 cm, respectively. Additionally, Megelski *et al.* were able to notice the formation of a beaded morphology for electrospun polystyrene fibers upon shortening of the distance between the capillary tip and the collector, which can be attributed to inadequate drying of the polymer fiber prior to reaching the collector [Megelski *et al.*, 2002].

- **Needle tip design and placement**

Several designs and configurations of needle tips have been investigated for the electrospinning process. For example, some researchers developed a coaxial, two-capillary spinneret. The use of multiple tips was also investigated [Ding *et al.*, 2004].

- **Collector composition and geometry**

A number of materials and geometries have been studied for the collection of electrospun polymeric fibers. Metal collectors, a water reservoir, and a methanol collector are usually used. They found that smooth fibers were obtained using the metal collector. Collection on the surface of water caused the hydrophobic polymer fibers to shrink, while methanol caused swelling of the fibers [Kim *et al.*, 2005]. It was found that the packing density was influenced by the conductivity of the collectors: the more conductive collectors dissipated the charge of the fibers. When this charge was not dissipated (non-conductive collectors), the fibers repelled one another, yielding a more porous structure [Liu *et al.*, 2002]. Fibers with a conductive frame produce better alignment than a non-conductive one. Fibers have also been collected using a rotating cylindrical drum collector rather than a stationary target (Fig. 1.2)

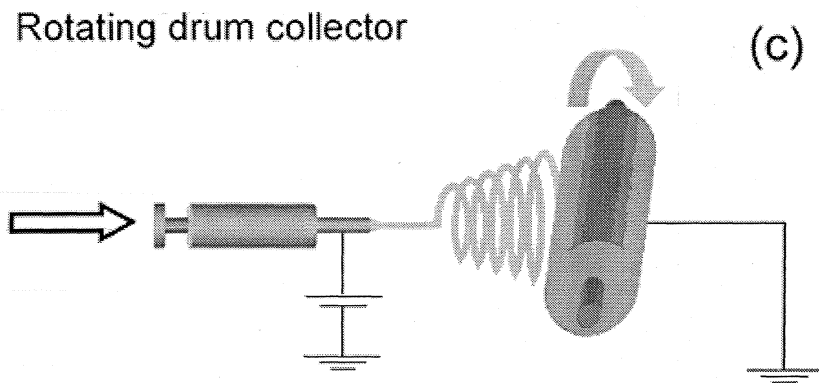


Fig 1.2 Electrospinning set up with rotating mandrel as collector

- **Ambient parameters**

Few studies have been conducted to examine the effects of ambient parameters (i.e., temperature and humidity) on the electrospinning process. Mit-Uppatham *et al.* spun polyamide-6 fibers at temperatures ranging from 25 to 60°C [Mit-Uppatham *et al.*, 2004]. They found that increasing the temperature yielded fibers with a decreased fiber diameter, and they attributed this decline in diameter to the decrease in the viscosity of the polymer solutions at increased temperatures. The humidity was varied by Casper *et al.* while spinning polystyrene solutions. Their work showed that increasing the humidity resulted in the appearance of small circular pores on the surface of the fibers; increasing the humidity further lead to the pores coalescing. Spinning has also been performed under vacuum in order to obtain higher electric fields; doing so produced fibers and yarns with larger diameters.

It is difficult to isolate the effect of many of the parameters since they are interrelated. For example, changing the solution concentration/viscosity affects other solution properties, such as the conductivity and surface tension. Additionally, though a large number of distinct polymers have been electrospun, there has been little systematic

investigation of the conditions required for successful spinning. A trial-and-error approach has been employed in which the solution properties and spinning parameters are varied until uniform, defect-free fibers are obtained. Electrospun polymer fibers have tremendous potential as tissue engineered scaffolds, and other applications.

1.2.2.2 Applications of Nanofibers

From a biological viewpoint, almost all of the human tissues and organs are deposited in nanofibrous forms or structures. Examples include: bone, dentin, collagen, cartilage, and skin. All of them are characterized by well organized hierarchical fibrous structures of nanometer scale. The current research in electrospun polymer nanofibers has focused one of their major applications on bioengineering. We can easily find their promising potential in various biomedical areas.

- **Medical prostheses**

Polymer nanofibers fabricated *via* electrospinning have been proposed for a number of soft tissue prostheses applications such as blood vessel, vascular grafts, guided tissue regeneration etc. In addition, electrospun biocompatible polymer nanofibers can also be deposited as a thin porous film onto a hard tissue prosthetic device designed to be implanted into the human body [Athreya & Martin., 1999]. This coating film with gradient fibrous structure works as an interphase between the prosthetic device and the host tissues, and is expected to efficiently reduce the stiffness mismatch at the tissue/device interphase and hence prevent the device failure after the implantation.

- **Wound dressing**

Polymer nanofibers can also be used for the treatment of wounds or burns of a human skin, as well as designed for haemostatic devices with some unique characteristics. With the aid of electric field, fine fibers of biodegradable polymers can be directly sprayed /spun onto the injured location of skin to form a fibrous mat dressing,

which can let wounds heal by encouraging the formation of normal skin growth and eliminate the formation of scar tissue which would occur in a traditional treatment . Non-woven nanofibrous membrane mats for wound dressing usually have pore sizes ranging from 500 nm to 1 mm, small enough to protect the wound from bacterial penetration *via* aerosol particle capturing mechanisms. High surface area of 5–100 m²/g is extremely efficient for fluid absorption and dermal delivery.

- **Drug delivery and pharmaceutical composition**

Delivery of drug/pharmaceuticals to patients in the most physiologically acceptable manner has always been an important concern in medicine. Drug delivery with polymer nanofibers is based on the principle that dissolution rate of a particulate drug increases with increasing surface area of both the drug and the corresponding carrier if needed. Ignatious and Baldoni described electrospun polymer nanofibers for pharmaceutical compositions, which can be designed to provide rapid, immediate, delayed, or modified dissolution, such as sustained and/or pulsatile release characteristics. As the drug and carrier materials can be mixed together for electrospinning of nanofibers, the likely modes of the drug in the resulting nanostructured products are: (1) drug as particles attached to the surface of the carrier which is in the form of nanofibers, (2) both drug and carrier are nanofiber-form, hence the end product will be the two kinds of nanofibers interlaced together, (3) the blend of drug and carrier materials integrated into one kind of fibers containing both components, and (4) the carrier material is electrospun into a tubular form in which the drug particles are encapsulated. The drug delivery in the form of nanofibers is still in the early stage exploration, a real delivery mode after production and efficiency have yet to be determined in the future.

- **Bone Tissue Engineering**

The search for successful bone analogue materials has led many researchers to prepare porous scaffolds with the intent to mimic as closely as possible the composition and/or

structure of the extracellular matrix (ECM) of natural bone. Electrospinning is a widespread technique for born tissue engineering. Bone tissue engineering, nanofibers from PCL have been extensively studied [Yoshimoto ET AL., 2003]. In addition to the pure PCL nanofibers, nanofibers from gelatin/PCL blend [Zhang et al., 2005] and PCL composite with calcium carbonate nanoparticles and hydroxyapatite (HAp) nanoparticles [Fujihara et al., 2005] for bone scaffolds have been investigated. The addition of 50% gelatin to PCL improved both the fiber mechanical strength and surface wettability, therefore enhancing the cell attachment and growth on the scaffold surface. Also, the cells were observed to migrate up to 114 μm inside the scaffold within one week of culture. In contrast, PCL nanofibers containing these inorganic nanoparticles were expected to have high osteoblast proliferation and differentiation. In addition, a bond-like calcium phosphate (CaP) was coated on PCL nanofiber surface [Wutticharoenmongkol *et al.* , 2006]. The CaP-coated nanofiber membrane showed high wettability. Because of its similar structure to the natural bone, such a mineralized electrospun scaffold is expected to be a potential cell carrier in bone tissue engineering. A combination of PCL nanofibers and microfibers was used to develop multilayer scaffolds [Tuzlakoglu *et al.*, 2005].

1.2.3 Polycaprolactone

Polycaprolactone is inexpensive biodegradable polyester and its molecular structure consists of five non-polar methylene groups and a single relatively polar ester group in repeated fashion. It has a low melting point of around 60°C and a glass transition temperature of about -60°C. PCL can be prepared by ring opening polymerization of ϵ -caprolactone using a catalyst such as stannous octanoate. PCL has good water, oil and solvent resistance.

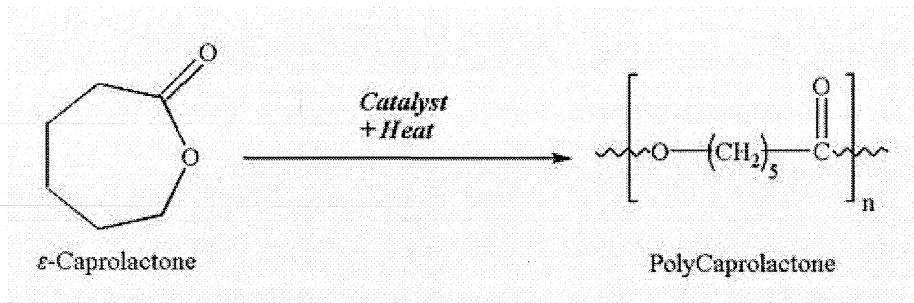


Fig 1.3 Conversion of caprolactone to polycaprolactone

PCL is a Food and Drug Administration (FDA) approved material that is used in the human body. It is regarded as a soft and hard tissue compatible material having wide applications in biomedical area such as resorbable, drug delivery system and recently bone graft substitutes. In dentistry (as composite named Resilon), PCL is used in root canal filling. It performs like gutta-percha, has the same handling properties, and for retreatment purposes may be softened with heat, or dissolved with solvents like chloroform. The quality which set PCL apart from other aliphatic polyesters is its low glass transition temperature (-60°C) making it flexible at physiological temperature and contributes to its high permeability for many therapeutic drugs.

Polycaprolactone, semi-crystalline linear resorbable aliphatic polyester, is subjected to biodegradation because of the susceptibility of its aliphatic ester linkage to hydrolysis [Kweona *et al.*, 2003]. Polycaprolactone, due to its slow degradation rate, is a good candidate to be used in bone scaffolding applications.

At present, PCL is regarded as a soft and hard-tissue compatible material including drug delivery system, and recently bone graft substitutes. However, applications of PCL might be limited because degradation and resorption kinetics of PCL. It is considerably slower than other aliphatic polyester due to its hydrophobic character and high crystallinity. Polycaprolactone is one of biomaterial used in bone repair. Marra *et al.* reported that PCL is a comparable substrate for supporting cell growth

resulting from two-dimensional bone marrow stromal cell culture. And, PCL/PLA blend disc incorporated with hydroxyapatite is feasible as scaffolds for bone tissue engineering.

PCL has good mechanical properties when it is biaxially stretched. Because of its inherent biodegradability and biocompatibility properties, PCL has been widely explored for its potential use in medicine, such as drug carriers, engineered skin, scaffolds for supporting the growth of fibroblasts and osteoblasts, etc. Its hydrophobicity often leads to unfavorable cell adhesion and growth. Therefore, the cytocompatibility of PCL should be further improved [Mattanavee *et al.*, 2009].

PCL, and their copolymers, are suitable materials for the design and fabrication of biocompatible scaffolds owing to their significant track record for regulatory approval, and their minimum provocation of inflammatory and immunological responses. They can have suitable surface chemistry for cell attachment, proliferation, and differentiation, and their degradation by-products are nontoxic and are usually metabolized and eliminated via natural pathways. Above all, these thermoplastic polymers can easily be processed into three-dimensional (3D) scaffolds with desired geometry and controlled porosity with interconnectivity [Christopher *et al.*, 2009]. Mechanical properties and non enzymatic degradation of PCL can be altered by regulating its crystal structure. Generally, it is rather hydrophobic and undergoes degradation very slowly by simple hydrolysis under human body conditions. The mechanical properties of PCL are similar to those of polyolefin owing to its high olefinic content.

Polycaprolactone is a soft- and hard-tissue compatible material including drug delivery system and is recently developed as a bone graft substitute. Its prospective use as a supportive scaffold material has been reported for a variety of tissue engineering applications including skin, bone, and mesenchymal stem cells. Jayarama Reddy Venugopal *et al* fabricate PCL and PCL-blended collagen nanofibrous membrane by electrospinning for wound dressing, cell adhesion and proliferation, and cell matrix

interaction, to produce allogeneic cultured dermal substitute (CDS) for skin defects and burn wounds.[Venugopal *et al.*,2006]

The culture of chondrocytes and osteoblasts on neat electrospun PCL fibers has also been reported. [Fujihara *et al.*, 2001]. Electrospun PCL tubes are used as scaffolds for tissue engineered blood vessel implants. In general, the electrospun PCL was found to exhibit rate dependence, as well as some dependence on the test temperature and on whether the sample was wet or dry. [Duling & Dupaix., 2008]

The advantage of electrospun PCL is that it is water resistant, biodegradable, and highly porous. Electrospinning provides pores that are heavily interconnected along with nanoscale fiber diameters. Perhaps the key advantage of nonwoven electrospun PCL over materials produced using a conventional fiber spinning process is in the size of the fibers that can be attained. Conventional processes typically produce fibers on the micron scale, whereas fibers produced via electrospinning are typically on the nanoscale. These smaller fibers lead to a morphology that is somewhat similar to the extracellular matrices seen in living organisms. PCL has low biodegradation rate due to its high degree of crystallinity can be mentioned as a main disadvantage. To increase the biodegradation rate, PCL is copolymerized or blended with polymers that biodegrade faster. If ϵ -caprolactone is copolymerized with ethylene oxide or poly(ethylene glycol) (PEG) to prepare PCL-PEG block copolymers, their hydrophilicity, biodegradability and mechanical properties can be improved, and thus they may find much wider applications. The large surface area of the polymer nanofibers with specific modifications facilitates cell adhesion and control of their cellular functions [Venugopal *et al.*, 2006].

1.2.4 Hydroxyapatite (HA)

Hydroxyapatite (HA), a major inorganic component of bone, has been used for biomedical implant applications and bone regeneration due to its bioactive, biodegradable, and osteoconductive properties [Sui *et al.*, 2007]. Being similar to the

mineral component of natural bone, they showed good osteoconductivity and bone bonding ability. However, whether used in block or granular forms, pure HA could not degrade in the human body. The nano size of the inorganic component (mainly bone-like apatite) in natural bone is considered to be important for the mechanical properties of the bone. In addition, nanosized HA may have other special properties due to its small size and huge specific surface area. Webster *et al.* have shown significant increase in protein adsorption and osteoblast cell adhesion on the nanosized ceramic materials compared to traditional micron-sized ceramic materials.

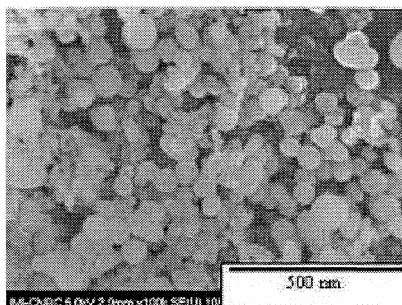


Fig 1.4 Nano hydroxyapatite cluster

Calcium phosphates are osteoconductive and bond directly to the bone. Hydroxyapatite $[\text{Ca}_{10}(\text{PO}_4)_6(\text{OH})_2]$, being the main mineral component of the bone, contributes to enhanced hydrophilic property of the biodegradable polymer and constitutes a natural substrate for cell growth. Hydroxyapatite is stable and resorbs at a slower rate than new bone formation. As a result, it is an ideal candidate as filler in polymer matrices for bioactive composites. The bioresorbability can be enhanced by using ionic doping agents or by reducing the size of the HAP crystals to nanometer scale. The reduction in particle size would result in improvement in cell adherence, sinterability, osteoconductivity, and a higher resorption rate.

Moncy V. Jose et al evaluated the effect of incorporation of nano-HA particles to the system. The morphology and mechanical properties revealed that, at low concentrations, nano-HA acted as reinforcement. However, at higher nano-HA loadings, it was difficult to disrupt aggregations and, hence, a detrimental effect was observed on the overall scaffold properties. Thermal analysis showed that there were slight interactions between the individual components even though the polymers existed as a two-phase system. Preliminary *in vitro* cell-culture studies revealed that the scaffold supported cell adhesion and spreading. The cells assumed a highly aligned morphology along the direction of fiber orientation. Protein adsorption experiments revealed that the synergistic effect of increased surface area and the presence of nano-HA in the polymer matrix enhanced total protein adsorption. [Jose *et al.*,2010]

The composite materials can provide superior structural properties such as high modulus and strength to weight ratios. To combine the osteoconductivity of calcium phosphates and biodegradability of polymer, polymer/ceramic composite have been developed for bone tissue engineering either by direct mixing or by biomimetic approach,[Liu *et al.*,1996 ,Kikuchi *et al.*,1997]. Composites of hydroxyapatite (HA) and biodegradable polymers such as polycaprolactone (PCL) are interesting materials for medical applications, especially for bone replacement. The composites were screened for cytocompatibility by a direct contact method, in view of the future application of these hydroxyapatite filled PCL polymers as scaffolds for bone engineering. [calandrelli *et al.*,2004].

1.2.5 Polyethylene Glycol

Polyethylene glycol is a condensation polymers of ethylene oxide and water with the general formula $H(OCH_2CH_2)_nOH$

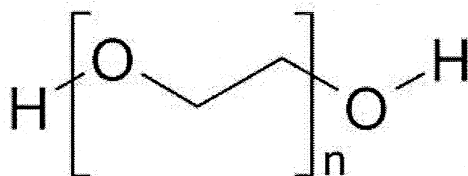


Fig 1.5 Polyethylene Glycol

Polyethylene glycol (PEG) is most widely used biocompatible polymer of chemical and biological application. Polyethylene glycol is a hydrophilic and nontoxic segment. [Cuong *et al.*,2008] Poly (ethylene glycol) (PEG) is a polymer well known for its low-fouling properties, biocompatibility, and solubility both in water and organic solvents. PEG has absence of antigenicity and immunogenicity, which allow PEG to be used for many clinical applications. Polyethylene glycol is not susceptible to hydrolysis, although its incorporation into the polymer backbone has been shown to enhance the rate of degradation by increasing hydrophilicity and, thus, water uptake. Polyethylene glycol containing copolymers have been proposed for tissue engineering and drug-delivery systems. For example, successful bone formation was observed *in vivo* during a three week study of cytokine-liberating PDLA-PEG-PDLA scaffold as reported by Saito *et al.* Polyethylene glycol containing amphiphilic copolymer may there for be useful to modify the surface of the biomedical polymer implants and to design the drug delivery system. Poly (ethylene glycol) hydrogels were investigated as encapsulation matrices for osteoblasts to assess their applicability in promoting bone tissue engineering.[Burdick *et al.*, 2002].

1.2.6 Copolymers

Synthetic block copolymers, has attracted increasing attention in the past decades due to its potential applications in biomedical fields, such as drug delivery, cell encapsulation, tissue repair. Block copolymers, as a result of their tunable phase separation behavior,

are key building blocks for a variety of functional nanostructured materials with potential applications ranging from electronic devices to drug delivery . In particular, triblock copolymers have been identified as important components for the fabrication of highly functionalized nanomaterials. As compared to AB diblock copolymers, ABA triblock copolymer allows for the incorporation of additional functionalities as well as a greater variety of tunable morphologies in thin films and in solution. Block copolymers are composed of long sequences ("blocks") of the same monomer unit, covalently bound to sequences of unlike type. The blocks can be connected in a variety of ways; schematics of AB diblock and ABA triblock structures



Hwang investigated the micellization and gelation of PEG–PCL–PEG triblock copolymers and suggested that the gelation of the copolymers seemed to be driven by micellar aggregation. PEG and poly (ε-caprolactone)(PCL) have been widely used in biomedical field, because they are both well-known FDA-approved biodegradable and biocompatible materials. The block copolymer system of PEG and PCL are compatible and biodegradable due to the enzymatic and pH dependent breakdown of ester bonds [Nie *et al.*, 2000]. Perret and Skoulios firstly prepared a series of block copolymers consisting of PEG and PCL, these ABA triblock copolymers containing PCL (A) blocks and PEG (B) blocks have been extensively studied. Martini et al. investigated the micellization and gelation properties of these triblock copolymers in aqueous solution, and they found the sol–gel transition on cooling such copolymer aqueous solution at given concentration. An et al. reported that the PCL-PEG-PCL system did not show lower gel–sol transition at any composition and the sol–gel transition on cooling. The crystalline nature of PCL is supposed to give the PEG-PCL-PEG triblock copolymer a brittle powder morphology in addition to the thermogelling property.

In recent years, Some researchers have reported the synthesis of multiblock copolymers of poly(ϵ -caprolactone)- poly(ethylene glycol) (PECL). Li et al. Reported the synthesis of PECL multiblock copolymers with high molecular weight (Mw: above 20 000) by the polycondensation of PEG bearing two carboxylic end groups and PCL diols in the presence of dicyclohexylcarbodiimide (DCC) as a condensing agent . Zhu and coworkers reported the synthesis of PECL triblock copolymers covering a wide range of PEG lengths via anionic polymerization of ϵ -CL with alkali metal alkoxide derivatives of PEG. Bogdanov et al. reported the synthesis of PECL copolymer by ring opening polymerization of PCL and PEG using stannous octoate as catalyst.

In this present study, we reported the preparation of triblock co-polymer, which composed of two hydrophilic segments (PEG) and one hydrophobic segment (PCL). The structure of triblock copolymers were characterized by ^1H NMR, FT-IR and differential scanning calorimetry (DSC). [Cuong *et al.*, 2008]

1.3 Gap

Poly (ϵ -caprolactone) (PCL) electrospun matrix has been reported as a scaffold for tissue engineering application. However, high hydrophobicity of PCL limits its use as functional scaffold. PCL, being hydrophobic, has slower degradation kinetics than other polyester family members such as poly (lactide), poly (glycolide) and poly (lactide-*co*-glycolide) thereby increases circulating half-life. The highly hydrophobic nature makes it unfavorable for cell adhesion and growth. An alternative and easy approach to modulate the hydrophilicity of the scaffold is by the incorporation of hydrophilic copolymers. In addition to the intrinsic hydrophobicity, the poor mechanical properties of PCL, depending on the preparation technique and molecular weight impair its use as material scaffold for hard tissue replacement. Therefore strategies to improve both hydrophilicity and mechanical performance of PCL based scaffolds are needed.

1.4 Hypothesis

Poly (ϵ -caprolactone) (PCL) and its copolymers form an important class of synthetic biodegradable and bioresorbable polymers.. However, its high hydrophobic nature and longer degradation time *in vivo* considerably restrain its potential applications .One of the main solutions for this problem is its copolymerization with other polymers having characteristic degradation rates and hydrophilicity. Blending of polycaprolactone with other hydrophilic polymers is also a good technique to modify its physical properties. Copolymers consisting of hydrophobic polycaprolactone blocks and hydrophilic polyethyleneglycol block have attracted the interest of material scientists in this regard. Polyethylene glycols are incompatible with polycaprolactone owing to their large difference in hydrophilic and hydrophobic nature.

The present study aims at synthesizing a triblock copolymer of the type PEG-PCL-PEG and further blended with PCL, which seems to be much more attractive and useful. The copolymer should be biocompatible with PCL and the inclusion of which supposed to increase the hydrophilicity and softness of the PCL without much decrease in mechanical properties. Also we can tailor the degradation rate by either increasing the molecular weight of the copolymer or varying the PCL/copolymer ratio. Herein we prepared scaffolds using PCL, PCL/ECE and their hydroxyapatite filled composite scaffolds by electrospinning technique, which is much more economic and industrially feasible process. Electrospinning technique can architecturally fabricate and mimic the chemical, physical and mechanical properties of the native extra-cellular matrix. It is supposed that the fibrous scaffolds produced using this technique has the potential to be used as tissue engineering scaffolds.

1.5 Objective

The ultimate objective of this work is to develop an innovative nano-structured polymer composite scaffold from bioresorbable electrospun nanofibers for bone tissue engineering applications.

The major steps are as follows:

- Synthesis of appropriate tri block co-polymer for the fabrication of nanofibrous composites scaffold.
- Chemical, Physical and thermal characterization of the tri block copolymer
- Solution blending of this tri block copolymer with PCL for improved degradation rate and hydrophilicity.
- Electrostatic co-spinning of this blend with nano-hydroxyapatite to fabricate nanocomposite scaffolds with varying spinning parameters.
- Characterization of the composite scaffold for its static and dynamic mechanical properties, porosity, morphology and biocompatibility.

In this work poly ethylene glycol is incorporated into the biodegradable polymer matrices polycaprolactone (PCL) to synthesize a triblock copolymer by appropriate chemistry to enhance the hydrophilicity and degradation rate. This triblock copolymer is then solution blended with PCL in DCM: DMF (80:20) to make a completely miscible solution. To this solution appropriate amount of reinforcement (HAP) is added and the composite scaffold developed by using electrospinning process. The scaffold was then characterized for its morphological and mechanical properties. Later the spinning parameters were varied and the effect of this variation on scaffold morphology was evaluated. The initial evaluation suggests us that this new material can act as a bespoke composite scaffold for bone tissue engineering application.

Chapter 2

Materials and methods

This chapter comprehends on the materials and methods used for the synthesis and characterization of ethylene glycol- ϵ -caprolactone – ethylene glycol (PEG-PCL-PEG) triblock copolymer its scaffold fabrication and characterization.

2.1. Synthesis of PEG-PCL-PEG (ECE) triblock co polymer

2.1.1. Materials

PCL diol with number average molecular weight, Mn 2000 (Sigma Aldrich), Polyethyleneglycol (PEG) with molecular weight 2000 (Merck Schuchardt), Hexamethylenediisocyanate (HDI) (Merck Schuchardt, Germany) were used in the present study. All the solvents used were of analytical grade and prior to use they were dried over CaH_2 and distilled under reduced pressure.

2.1.2. Method

The PEG-PCL-PEG triblock copolymer was synthesized by two step reaction.

Step 1: Functionalization of telechelic PCL diol with HDI

The synthesis of NCO- terminated PCL prepolymer was performed in solution under N_2 atmosphere. Hexamethylene diisocyanate and dry toluene were placed into a 250 ml two necked flask connected with a condenser at $60\text{-}65^\circ\text{C}$. PCL diol dissolved in dry toluene were added to HDI slowly for a period of 1 hr at $60\text{-}65^\circ\text{C}$. The ratio of NCO/OH was 2:1 (mol/mol). The reaction mixture was heated to $80\text{-}85^\circ\text{C}$ and the reaction was continued for 24 hrs. The product was stored at moisture free condition at a temperature less than 6°C .

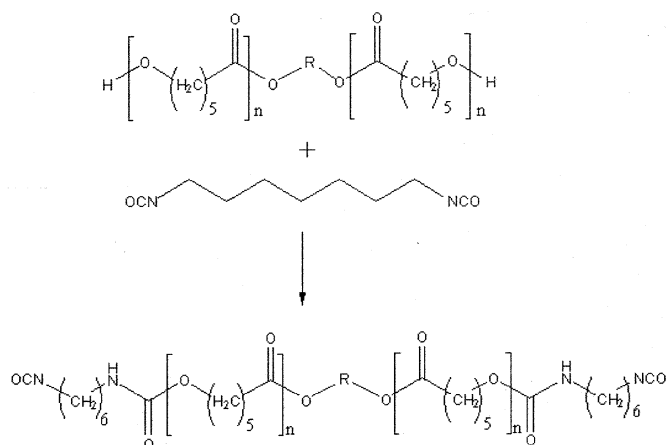


Fig 2.1 Functionalization of telechelic PCL diol with HDI

Step 2: Synthesis of ECE

The triblock copolymers were synthesized from a carbamoyl derivative of telechelic PCL and HDI with molar ratio of PEG to the prepolymer 2:1 (mol/mol).

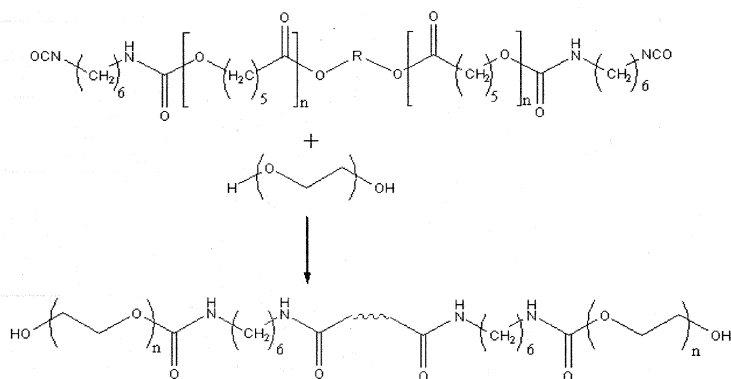


Fig 2.2: Synthesis of ECE

Dry PEG dissolved in dry toluene were placed into a 250 ml two necked flask connected with a condenser at 60-65⁰C. PCL prepolymer dissolved in toluene was added into the reaction vessel slowly drop wise with constant stirring for over a period of 60 min. The reaction mixture was kept under stirring at 80⁰C for 36 hours. The product was isolated by dissolving the reaction mixture in dichloromethane, followed by precipitation in hexane at 0⁰C.

2.2 Characterization of the PEG-PCL-PEG (ECE) triblock co polymer

2.2.1. Chemical Characterization

2.2.1.1. Nuclear magnetic resonance analysis (¹H-NMR)

Nuclear magnetic resonance (NMR) is a powerful and versatile spectroscopic technique for investigating molecular structure and dynamics. It involves reorientations of nuclear spins with respect to an applied static magnetic field. This spectroscopy uses radio waves to obtain information about how atoms are connected in compounds. The ¹H-NMR spectra were recorded on 300-MHz Bruker NMR spectrophotometer in CDCl₃, containing small amount of TMS as internal standard.

2.2.1.2. Fourier transformation infrared spectroscopy (FTIR)

Fourier transformation infrared (FTIR) spectroscopy is one of the most common and widely accepted spectroscopic techniques for the investigation of functional groups. IR radiation causes the bonds in molecules to vibrate. This spectroscopy exploits the fact that molecules absorb specific frequencies of IR radiation that are characteristic of their structure. By interpreting the infrared absorption spectrum, the functional groups in a molecule can be determined. The synthesized prepolymer and copolymer was scanned in the range of 400 to 4000 cm⁻¹ in a Nicolet 5700 FTIR Spectrometer.

2.2.2. Physical Characterization

2.2.2.1. Gel permeation chromatography analysis (GPC)

Gel permeation chromatography (GPC) is a macro molecular separation technique used to determine the molecular weight and molecular weight distribution of the polymer. GPC was used to calculate the number average molecular weight (M_n), weight average molecular weight (M_w) and poly dispersity index (M_w/M_n) for polymer samples. A molecular weight distribution profile was made for each of the polymer, and the column efficiency is calculated. The column efficiency is inversely proportional to the column radius and the analysis time is directly proportional to the column radius. GPC measurements of the synthesized copolymer (ECE) was carried out by using a .05% polymer solution in Waters HPLC system, 600 series pump with tetrahydrofuran (THF) as the mobile phase with a flow rate 1ml/min and polystyrene standards of molecular weight (100000/34300/3250).

2.2.3. Thermal Characterization

2.2.3.1. Thermogravimetric analysis (TGA)

Thermogravimetric analysis (TGA) is a thermal analysis technique used to measure changes in the weight of a sample as a function of temperature and /or time. TGA is commonly used to determine polymer degradation temperature, residual solvent levels, absorbed moisture constant, and amount of inorganic (non-combustible) filler in polymer or composite material composition. A simple explanation of TGA sample evaluation may be described as follows. The sample is placed into a tarred sample pan, which is attached to a sensitive micro balance assembly. The sample holder position of TGA balance assembly is subsequently placed into a high temperature furnace. The balance assembly measures the initial sample weight at room temperature and then continuously monitors the changes in the sample weight as heat is applied to the sample. TGA test may be run in a heating mode at some controlled heating rate, or isothermally. Typical weight loss profiles are analyzed for the amount or percentage of weight loss at

any given temperature, the amount of percentage of noncombustible residue at some final temperature, and the temperature of various sample degradation processes.

TGA was carried out based on the ASTM E 1131-08 standard using SDT-2960(simultaneous DTA-TGA) manufactured by TA instrument Inc. USA. The test was conducted in nitrogen atmosphere using calcined alumina as reference material. The temperature range used was from room temperature to 600°C at a the heating rate of 10°C/min

2.2.3.2 Differential Scanning Calorimeter (DSC)

Differential scanning calorimetry or DSC is a thermoanalytical technique in which the difference in the amount of heat required to increase the temperature of a sample and reference are measured as a function of temperature. Both the sample and reference are maintained at nearly the same temperature throughout the experiment. Generally, the temperature program for a DSC analysis is designed such that the sample holder temperature increases linearly as a function of time. The reference sample should have a well-defined heat capacity over the range of temperatures to be scanned.

The basic principle underlying this technique is that, when the sample undergoes a physical transformation such as phase transitions, more or less heat will need to flow to it than the reference to maintain both at the same temperature. Whether less or more heat must flow to the sample depends on whether the process is exothermic or endothermic. By observing the difference in heat flow between the sample and reference, differential scanning calorimeters are able to measure the amount of heat absorbed or released during such transitions. DSC may also be used to observe more subtle phase changes, such as glass transitions. It is widely used in industrial settings as a quality control instrument due to its applicability in evaluating sample purity and for studying polymer curing.

DSC was carried out based on the ASTM E 537-07 using DSC-2920 (Differential Scanning Calorimeter) manufactured by TA instrument Inc. USA. The temperature range used was from -50°C to 600°C at a the heating rate of 10°C/min

2.3. Characterization of Hydroxyapatite

2.3.1. Particle size analysis

Particle size analysis of hydroxyapatite (Spray dried hydroxyapatite (HAP) obtained from Bioceramics laboratory, SCTIMST) was measured by a particle size analyzer, Zetasizer (Nano ZS, Malver Instruments ,UK). The suspension of the particle is prepared in water and the zetasizer system determines the size by first measuring the Brownian Motion of the particle in the suspension using dynamic light scattering and interpreting the size using Stark Einstein equation given below.

$$D_H = KT / (3\Pi\eta D)$$

Where,

D_H = hydrodynamic diameter

K = Boltzman constant

η = solvent viscosity

T = absolute temperature

D =diffusion coefficient

The suspension is taken in a cuvette and readings are taken with the nanosizer fitted with a 633nm laser. The diffusion coefficient and hydrodynamic diameter (particle size) are calculated by dispersion technology software version 5 from the correlation curve.

2.4. Fabrication of scaffold

Scaffolds were fabricated using electro spinning technique. This process, invented by Formhals(1)in 1934, operates on the basis that the application of a high voltage to a viscous polymeric based solution results in the accumulation of charges on the solution which forces the solution to stretch and form a jet of charged fibrous structures as a direct consequence of repulsion forces. The applied voltage for operation may vary according to polymer solution. Voltage is high enough to break the surface tension of polymer solution and droplet formed at the end of the syringe inducing the formation of a fiber jet.

In parallel an electrostatic field is created between the needle and the collector, and is used to direct the charged fibers to the selected area. Virgin scaffolds were fabricated using PCL (Mn 80,000) as synthetic biodegradable polymer, and also with blends of PCL and the synthesized triblock copolymer ECE. Nano-hydroxyapatite filled composite scaffolds were also prepared with PCL and PCL-ECE blends. The concentration of nano-HAP (0.5, 1, 2, 4 and 6 wt %) as well as the PCL to copolymer ratio was selected with respect to mechanical testing.

2.4.1. Preparation of Spinning dopes

Spinning dopes were prepared by dissolving a weighed amount of PCL pellets in a solvent mixture of dichloromethane and dimethyl formamide by vigorous stirring. For the multi- component system, a two step method was used for the dispersion of the HAP in the polymer solution. Initially, HAP was dispersed in DCM and ultrasonicated at room temperature for 90min to disrupt possible agglomerates. In the second step, the appropriate weight of PCL, ECE and sufficient quantity of DMF were added to the HAP/DCM dispersion. This was followed by magnetic stirring until the polymer dissolved completely and 90 min of ultrasonication (microclean-103) to obtain a uniform dispersion of the nanoparticles in the polymer solution. Prior to electrospinning, the spinning dopes were characterized for its conductivity and viscosity by using a PC Scan

300 conductivity meter (Eutech instruments) and Brookfield Programmable DV II + viscometer respectively. All measurements were carried out at 25 ± 1 °C

2.4.2. Electrospinning process

The solutions were electrospun in air using a DC voltage power supply (Gamma High Voltage Research) operated at 7–20 kV, a programmable syringe pump (KD Scientific, model 200) , and a grounded stainless steel collecting drum connected to a high speed motor.

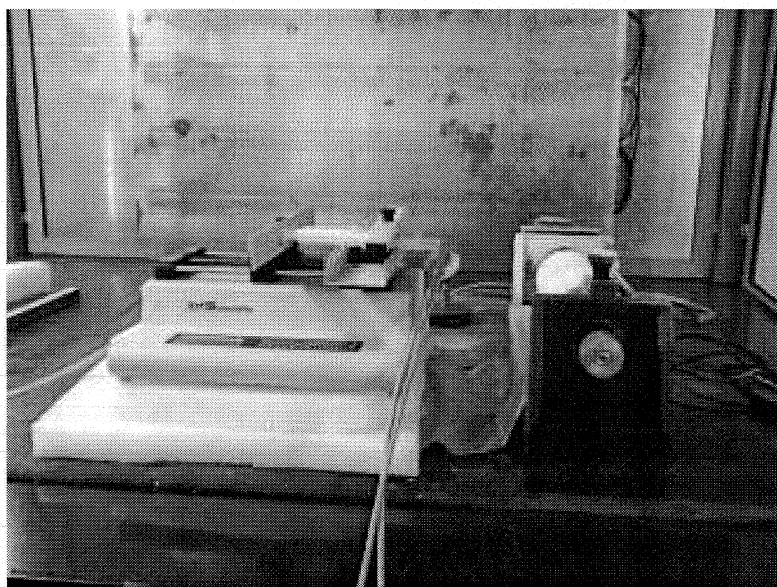


Fig 2.3 Electrospinning apparatus

Aligned fibers of blend and multi-component system were spun and deposited on the collector rotating at a speed of 500rpm. A 21 gauge syringe needle was used in the setup and placed 15cm away from the collector drum. A voltage in the range of 12-14kV was applied to the needle and the syringe pump was set at a flow rate of 2ml/h. All solutions were ultrasonicated for 1 hr prior to electrospinning to improve suspension of HA particles in the polymer pre-spinning solution. . The collection time for the above

process was fixed about 7hrs and the thickness of the sample obtained was noted. After the process, the electrospun fibers were dried in vacuum oven at 40⁰ C for about 48 hrs to remove the residual solvent.

2.4.3. Characterization of scaffolds

The morphology of electrospun fibers is influenced by various processing parameters such as concentration of the polymer solution, applied voltage, feeding rate, distance between the needle tip and the collector. Hence in the present work, effects of certain parameters are evaluated.

- ✦ Effect of PCL concentration (8, 10, 12, 15 and 20 %).
- ✦ Effect of weight % of HAP on PCL (0.5, 1, 2, 4 and 6 wt- %).
- ✦ Effect of PCL/ECE ratio (90: 10, 80:20 and 70: 30).
- ✦ Effect of applied voltage (12, 15, 17 and 20 kV)
- ✦ Effect of flow rate (0.5, 1, 2 ,3 and 4 ml/hr)
- ✦ Effect of DCM /DMF solvent ratio (90:10, 80:20, 70:30 and 60:40).

2.4.3.1. Morphological observation using Scanning Electron Microscopy (SEM)

Scanning electron microscope (SEM) an instrument that images the sample surface by scanning it with a high-energy beam of electrons in a raster scan pattern. The electrons interact with the atoms that make up the sample producing signals that contain information about the sample's surface topography, composition and other properties such as electrical conductivity. The surface morphology of the electrospun fibers were observed under a scanning electron microscope (JEOL, JSM-6390, model 7582, Japan) as well as (Hitachi, Japan, S2400). . The samples were sputter coated with platinum and imaged at an accelerating voltage of 20 kV. The fibre alignment as well as fiber smoothness was analyzed from the SEM micrographs. The average fiber diameters, standard deviation were evaluated using Image J software from 60 different positions.

2.4.3.2. Mechanical Characterization using UTM & DMA

The mechanical property of a scaffold is an important aspect. The purpose of scaffold is not only for providing a surface for cell residence but also for maintaining mechanical stability at the defect site of the host. It must provide sufficient biomechanical support during the process of tissue regeneration and degradation.

✦ Universal Testing Machine(UTM)

A universal testing machine, also known as a materials testing machine or materials test frame, is used to test the mechanical properties such as tensile stress, modulus and %elongation. Mechanical properties of electrospun fibrous membranes were determined with a tabletop Universal testing machine (Instron 3345, single column, UK) with the use of a 10N load cell under a cross-head speed of 10 mm/min at ambient conditions.

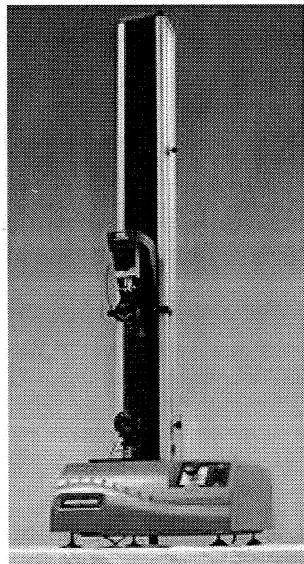


Fig 2.4 Universal Testing Machine

A universal testing machine, also known as a materials testing machine or materials test frame, is used to test the mechanical properties such as tensile stress, modulus and %elongation. Mechanical properties of electrospun fibrous membranes were determined with a tabletop Universal testing machine (Instron 3345, single column, UK) with the use of a 10N load cell under a cross-head speed of 10 mm/min at ambient conditions. All samples were prepared in the form of rectangular strip with dimensions of 50×5 mm. The thicknesses of samples were measured at 5 different locations along the span length using a digital micrometer having a precision of $1 \mu\text{m}$ and an average taken. At least six set of specimens were tested both longitudinally as well as transversely for each type of electrospun fibrous scaffolds.

✦ **Dynamic Mechanical Analysis (DMA)**

Dynamic mechanical analysis is a technique used to study the viscoelastic nature of polymer. It is a non destructive test technique in which an oscillatory stress is applied to the sample and the resultant strain determines as a function of both frequency and temperature.

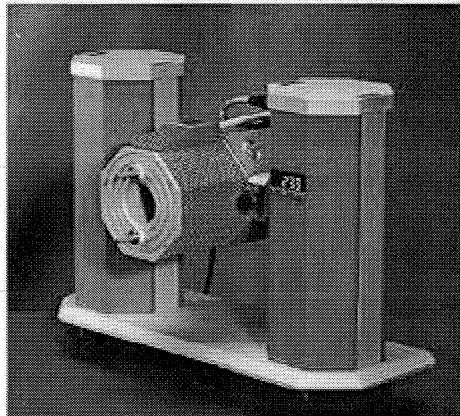


Fig 2.5 DMA

From dynamic mechanical analysis a comprehensive knowledge of the relationship between the various viscoelastic parameters such as a storage moduli, loss moduli, mechanical damping parameter or tan delta against the temperature and time may be obtained. Dynamic modulus and storage modulus reflects the stiffness of the material. Loss modulus is a measure of the mechanical damping or internal friction proportional to the energy transformed into heat during a deformation cycle. The storage modulus and tan delta of the PCL, PCL/ECE with and without hydroxyapatite as a function of temperature at a frequency of 1 Hz were determined by Triton DMA (Tritec 2000 B, Triton Technology Limited, UK) in the tension mode from -100°C to 40°C. Rectangular sample of 4 x 0.4 x 0.06 mm was used for the test.

2.4.3.3. Porosity measurement using Micro-Computed Tomography analysis (μ -CT)

Porosity is a key factor which determines cell seeding efficiency, diffusion and the mechanical strength of the scaffold. High porosity and high surface area to volume ratio are required for uniform cell delivery, cellular attachment and neo-tissue in growth. The 3D structural and architectural information as well as the pore size distribution of the electrospun fibrous scaffolds was assessed by means of microcomputed tomography analysis using Scanco 40 equipment (μ -CT 40, Scanco Medicals, Switzerland).

2.4.3.4. In-Vitro degradation tests in phosphate buffer saline (PBS)

Rectangular specimens ($20 \times 20 \times 0.1 \text{ mm}^3$) were weighed and placed in closed bottles containing 30mL phosphate buffer solution pH: 7.4 (shown in Appendix) and incubated *in-vitro* at $37 \pm 2^\circ\text{C}$ in shaking water bath for different time periods (2, 7, 14 and 28 days). To maintain the PBS activity, the solution was changed every 2 days for the first week and thereafter every week. At the end of each degradation period, specimens were withdrawn from the incubator and blotted with tissue. The aged specimens were characterized for surface morphological and mechanical properties using Scanning Electron Microscope (JEOL, JSM-6390, model 7582, Japan) and Universal testing

machine (Instron 3345, single column, UK) respectively to evaluate the biodegradation behavior .

2.4.3.5. Cytotoxicity evaluation using MTT assay

The viability of attached cells on the scaffold was confirmed by MTT [3-(4, 5-Dimethylthiazol -2-yl)-2, 5- diphenyl tetrazolium bromide] assay. This assay is based on the ability of viable cells to reduce a tetrazolium based compound, MTT, to a purple formazan product. The material extract was prepared by incubating test material with culture medium containing serum at 37 ± 2 ° C for 24 to 26 hrs at an extraction ratio of $6\text{cm}^2/\text{ml}$. The extract (100%) was diluted to 50% and 25% with culture medium. 100% extract prepared using HDPE was considered as negative control. Extract and control medium were added to subconfluent monolayer of L-929 cells in triplicate in a 96 well culture plate and incubated at 37 ± 2 ° C for 24 ± 2 hrs. Extract and control medium was replaced with 200 μl fresh culture medium to which 50 μl MTT (1mg/ml in serum free medium) was added. Cells were incubated at 37°C for 2hrs. After discarding the MTT medium, 200 μl of isopropanol was added to all wells and mixed. The color developed was quantified by measuring absorbance at 570 nm using a micro plate reader (Biotek).

Chapter 3

Results and Discussion

The chapter comprehends on the results obtained from various studies. In the present work, synthesis of a triblock copolymer consisting of non-toxic, biocompatible and hydrophilic polyethylene (PEG) blocks and biodegradable, hydrophobic polycaprolactone (PCL) block of the type PEG-PCL-PEG (ECE) was successfully synthesized by a reaction of coupling. The yield of prepared copolymer was about 72%. The synthesized copolymer was blended with hydrophobic PCL in order to improve its mechanical properties and to introduce hydrophilicity thereby tailoring its degradation profile. Fibroporous scaffolds via electrospinning technique using PCL as well as with blends of PCL and ECE were successfully fabricated. Nanohydroxyapatite filled fibrous scaffolds were also fabricated with PCL and PCL/ECE and it was evaluated alongside with neat PCL and PCL/ECE blends for its static and dynamic mechanical properties, thermal stability, fiber morphology, biostability and cytocompatibility.

3.1. Fourier Transformation Infrared Analysis (FTIR) of NCO Terminated PCL

Prepolymer and the triblock copolymer ECE

FTIR spectroscopy was used to characterize the structure of the obtained prepolymer. The FTIR spectrum of prepolymer is shown in figure 3.1. The band at 3387 cm^{-1} was assigned to the N-H groups bonded with carbonyl ($\text{N-H}\dots\text{O}=\text{C}$) in the prepolymer. The C-H stretching vibrations were observed at 2944 cm^{-1} . The band at 1525 cm^{-1} is attributed to the overlapping of a signal for the N-H, N-C bands and NCO group. The NCO peak at 2271.8 cm^{-1} confirms the completion of the reaction in step 1.

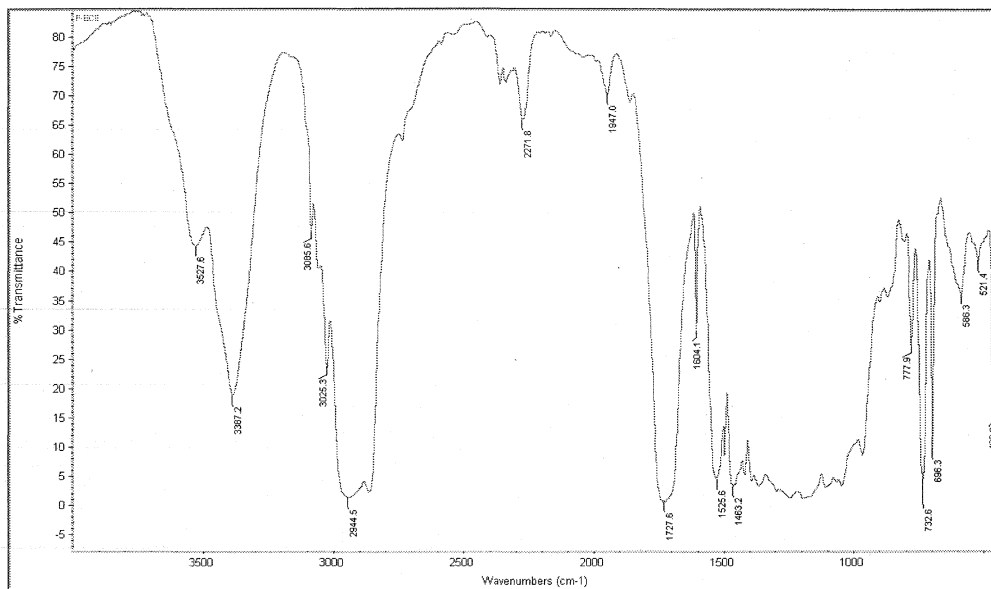


Fig 3.1 FTIR spectrum of the NCO terminated PCL prepolymer

The structure of synthesized triblock copolymer is confirmed by FTIR spectra (Fig 3.2). The absorption band at 1148 cm^{-1} is attributed to the characteristic C-O-C stretching vibration of the repeated $-\text{OCH}_2\text{CH}_2-$ units of polyethylene glycol backbone. A weak C=O stretching band at 1724 cm^{-1} determines the presence of $-\text{C}(\text{O})\text{OCH}_2-$ ester bonds in the repeated units of the PCL. There is no absorption peak in the range $2270 - 2285\text{ cm}^{-1}$ which indicates that the NCO- groups of hexamethylene diisocyanate have disappeared completely. The weak absorption band at 1531 cm^{-1} N-H bending vibrations confirms the formation of urethane group in the copolymers.

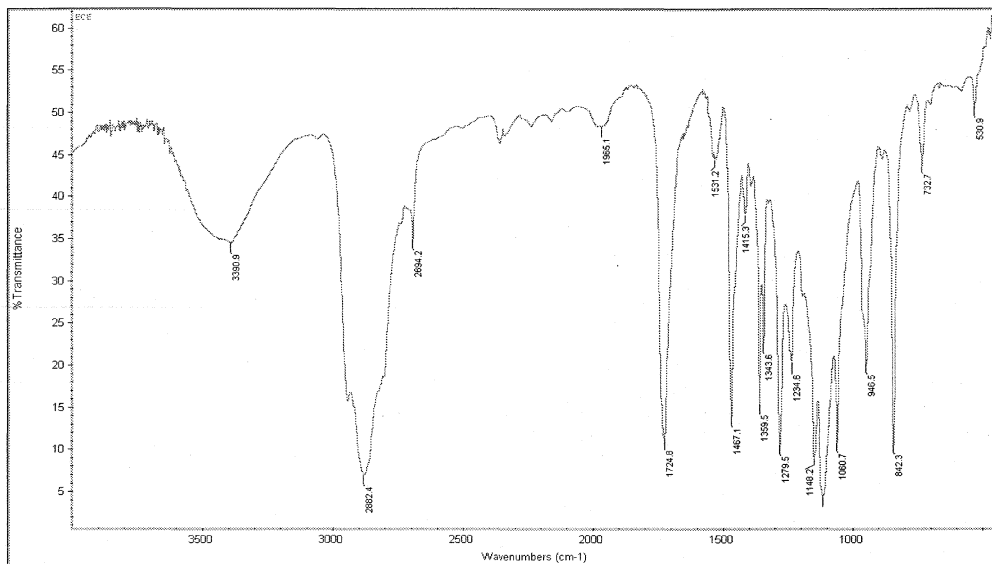


Fig 3.2 FTIR spectra of copolymer ECE

3.2. Nuclear Magnetic Resonance Spectroscopy of ECE copolymer

The ^1H NMR spectra also confirmed the formation of PEG-PCL-PEG triblock copolymer.(fig 3.3).

The appearance of the strong signal due to the α -, β -, γ -, δ - and ϵ -methylene protons to the carbonyl group of the PCL side chain was detected at 2.28 ppm, 1.62 ppm, 1.38 ppm and 4.03 ppm, respectively. A broad singlet signal of the poly (ethylene glycol) back bone at 3.65 ppm is also observed. The signal at 3.16 ppm is attributed to the NH and CH_2 -NH protons in the urethane group. The signals at 4.03 ppm are attributed to the $-\text{NH}-\text{C}(\text{OO})\text{O}-\text{CH}_2$ protons.

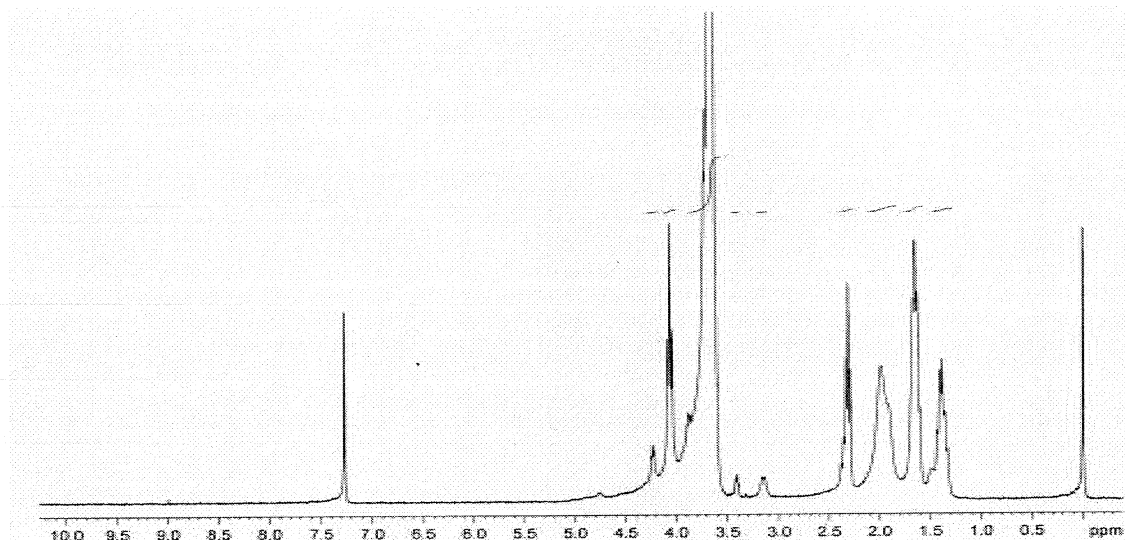


Fig 3.3: ^1H NMR spectra of the PEG-PCL-PEG triblock copolymer

3.3 Gel Permeation Chromatography analysis of ECE copolymer

The average molecular weight and polydispersity index (PDI) were measured by GPC using THF as an elution solvent and monodisperse poly (styrene) as standard. The copolymer showed a monomodal narrow molecular weight distribution with PDI 1.038. The number average (\overline{M}_n) and weight average (\overline{M}_w) molecular weights obtained are respectively 14662 and 15213. The GPC curve of the synthesized copolymer is shown in fig 3.4

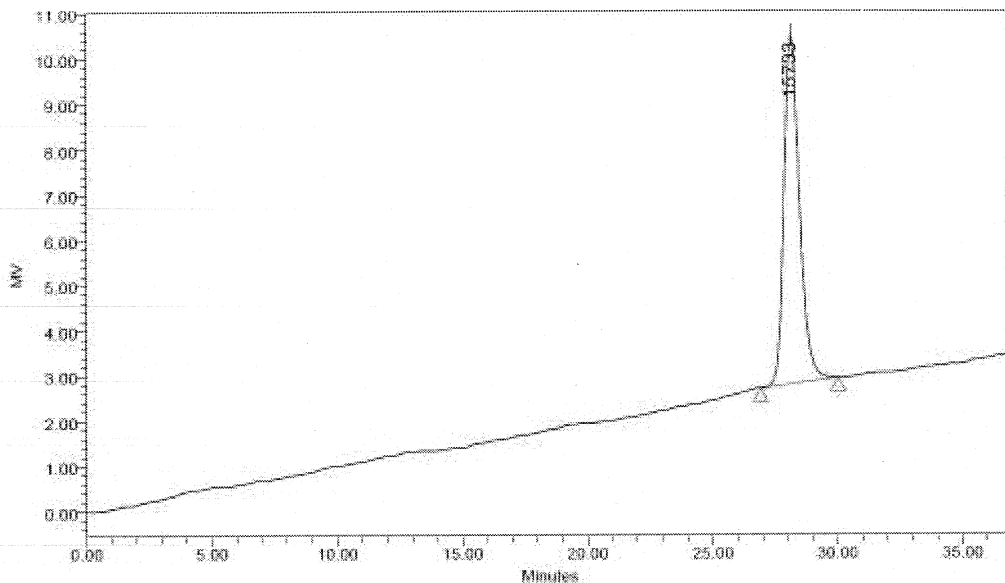


Fig 3.4 GPC analysis of ECE

3.4. Thermogravimetric analysis (TGA) of ECE copolymer

Thermogravimetric analysis provides information about the decomposition mechanism of materials. It gives information about the nature and extent of degradation of the material. The TGA curve of synthesized copolymer is shown in Fig.3.5. The copolymer is thermally stable up to 201°C. A two step degradation profile was observed for the copolymer probably due to the two blocks present in the polymer and the temperature at which 50% degradation occurred was at 387 °C.

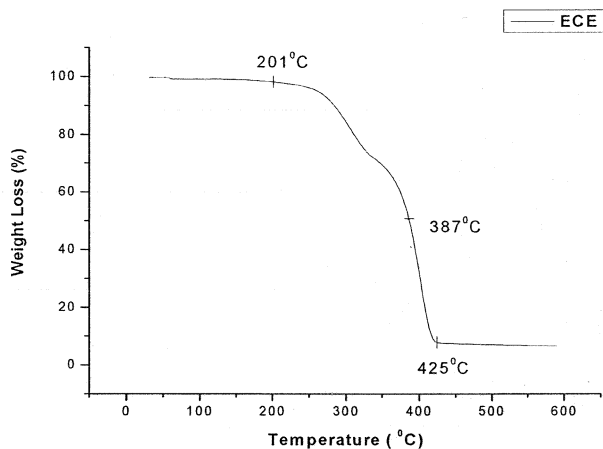


Fig 3.5 TGA of copolymer ECE

3.5. Differential Scanning Calorimetric (DSC) analysis of copolymer ECE

The thermal change of the synthesized copolymer was assessed using differential scanning calorimeter. The DSC curve of the copolymer is shown in fig 3.6. The copolymer showed an endothermic peak at 51°C which corresponds to T_m .

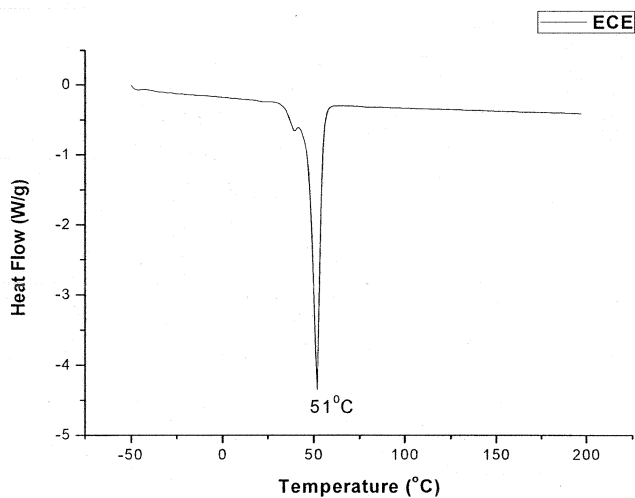


Fig 3.6 DSC of copolymer ECE

3.6 Characterization of Hydroxyapatite (HAP) using Particle size analyzer

The size distribution of the hydroxyapatite particles used in the present study was analyzed using particle size analyzer. The particle size was measured with regard to the volume of particles in the sample. On volume basis the average particle size is taken to be the size of particles occupying the maximum volume. The average particle size of HAP particles was found to be 90 nm and the polydispersity index was 0.292

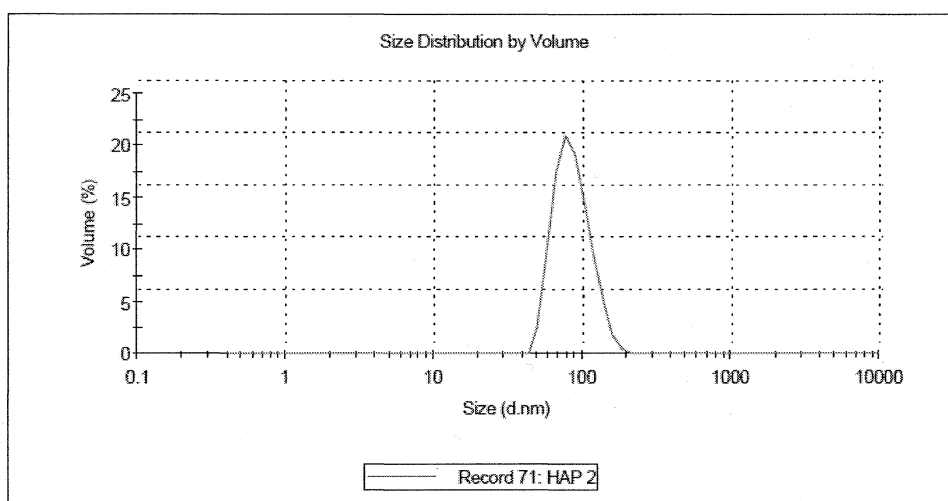


Fig 3.7 Particle size distribution of HAP

3.7 Fabrication & Characterization of Scaffolds

Initially, the optimum concentration needed for fibre formation was determined by spinning PCL at different concentration. Based on its morphological and mechanical evaluation, the polymer concentration was optimized. Further, the effect of incorporating bioactive filler HAP as well as hydrophilic triblock copolymer ECE on mechanical properties and fibre diameter is evaluated.

3.7.1. Effect of PCL concentration

The effect of solution concentration on the fiber morphology, average fiber diameter and mechanical strength was studied for five different concentrations of PCL solution (8, 10, 12, 15 and 20 wt %). Electrospinning of neat PCL with different concentration was performed under same conditions (i.e. 12 kV voltages, 15cm distance from needle tip to mandrel, 2ml/h flow rate and mandrel rotation of 500 rpm). The morphology of the electrospun fibres at different polymer concentrations are shown in Fig 3.8.

For 8 wt % solution, big spherical beads in combination with thin fibers were observed (Fig.3.8a). Spherical beads can be produced by electrospinning of dilute polymeric solutions. If the solvent does not evaporate completely before the spherical beads reach the collector, some of the particles can agglomerate. The breakdown of the jet into droplets may be favored at low molecular weights in the polymer and at low concentrations in the solution. Solid beads were generally obtained at relatively low rates of solvent evaporation and small deposition distances (i.e., distance from the tip of the needle to the collector). Rapid solvent evaporation from a drop of solution may lead to the development of a thin skin of polymer on the surface. This skin layer reduces the rate of evaporation of the solvent because of diffusion barriers. When the organic solvent inside the bead finally escapes, the atmospheric pressure tends to collapse the particle. As a result, cavities are formed on the surface of the particle. (Chen-Ming Hsu & Shivkumar, 2004).

Samples with fine fiber structure were observed for all other concentrations (Fig. 3.8 b-d). In this images fibers were generally straight (indicating significant elongational flow) with a round cross section. These fibers are typically observed when the solvent has evaporated completely before reaching the collector. When the concentration is increased to 20% the fiber surface thickens and exhibits a characteristic waviness as shown in Fig 3.8(e). These surface undulations may lead to instabilities in the jet which may promote splitting and branching.

The gradual increase in fiber diameter also can explain on the basis of viscoelastic behavior of polymer solutions. In dilute solutions, the polymer chains are sufficiently isolated and do not overlap. At a critical concentration, c^* , the polymer-polymer interaction starts to become significant. At $c > c^*$, the formation of entanglements between molecules leads to a dramatic increase in viscosity. With increase in viscosity elongation of fiber in applied electric field decreases as a result the increment of fiber diameter occurred.

The formation of beaded structures during electrospinning is fairly common and has been reported by several investigators. Small beads can disassociate from the jet if the capillary instability driven by surface tension is prevented by significant viscoelastic stresses. Although the exact reasons for bead formation are not clear, it has been shown that the viscoelasticity of the solution, charge density in the jet, and the surface tension of the solution are the key factors that control this behavior. At low solution viscosities (i.e., low concentrations), the beads are typically spherical, while spindle-like beads are observed at high viscosities (or concentrations).

The solution concentration has a significant effect on the fibre morphology. Thus, there is an upper and lower limit for solution concentration during electrospinning, corresponding to the level of entanglement between the polymeric chains. This minimum and maximum concentration will depend on the molecular characteristics of the polymer. i.e., molecular weight, polydispersity, branching etc.).

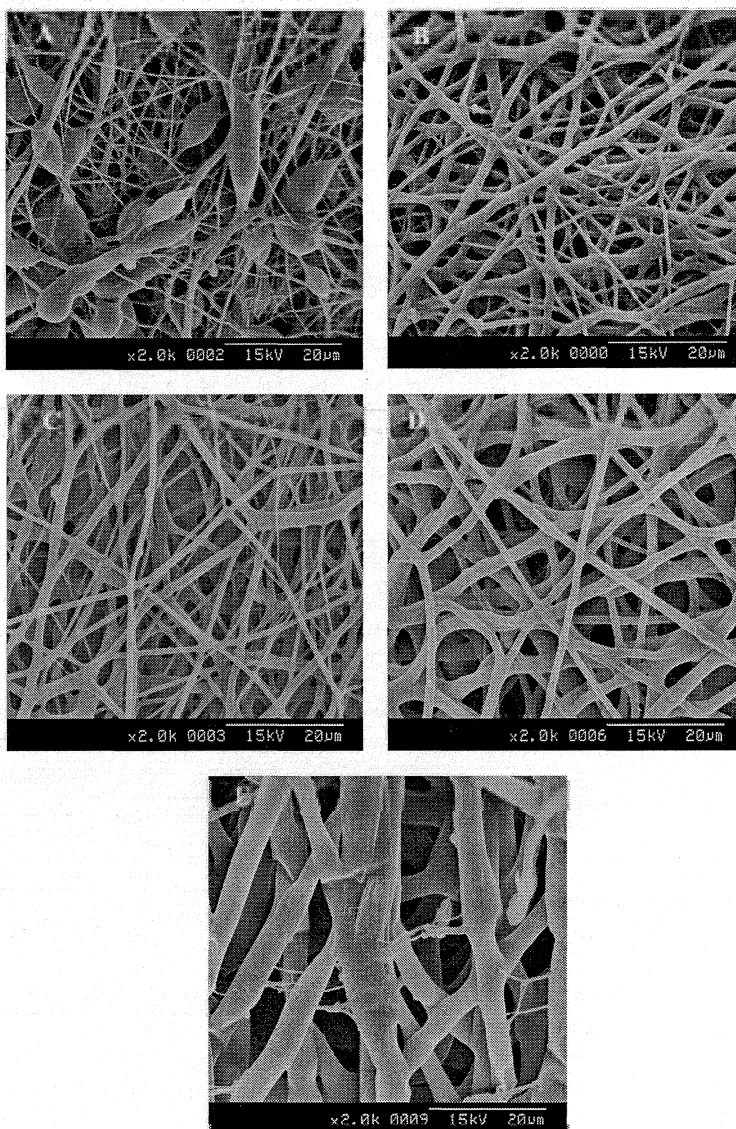


Fig 3.8: SEM micrographs of the electrospun PCL samples at different concentrations; (A) 8% (B) 10% (C) 12% (D) 15% and (E) 20%

Table 3.1 shows the dependence of the average fiber diameter as well as tensile strength on the solution concentration. In all cases the increment of the solution concentration resulted in the increase of the average fiber diameter, which may be due to the increased concentration enabled the charged jet to withstand a larger stretching force (from Columbic repulsion). These findings were observed in many studies and were attributed to the solution viscosity, which is proportional to the solution concentration. It must be noted that beaded fibers relatively indicate lower mechanical strength as compared to fine surface fibers (Inai et al.). As PCL scaffolds require mechanical stability, formation of beaded fibers should be avoided. The mechanical properties of electrospun samples are also be analyzed and the results are summarized in the Table 3.1.

Concentration (%)	Fiber diameter (μm)	Tensile strength (MPa)	
		Longitudinal	Transverse
10	0.54 ± 0.2	6.5 ± 0.4	3.9 ± 0.3
12	0.65 ± 0.2	5.6 ± 0.5	4.0 ± 0.5
15	0.71 ± 0.2	4.1 ± 0.2	3.0 ± 0.2
20	1.98 ± 0.4	3.5 ± 0.4	2.9 ± 0.6

Table 3.1 Effect of solution concentration on fiber diameter and tensile strength

From the above observations, we could find that as the polymer concentration increases the tensile strength decreases. This is due to the increase in fiber diameter of electrospun scaffold. Electrospun fibers at 10 wt % polymer concentration seem to have better mechanical strength and fiber diameter.

3.7.2 Effect of filler content

The effect of concentration of HAP on mechanical properties of neat PCL is evaluated. Mechanical properties of PCL/HAP composite electrospun scaffolds with different weight percentages of HAP (0.5, 1, 2, 4 and 6 wt %) are shown in fig 3.9. The amount of HAP incorporated may be a critical factor to determine overall morphology of nanofibers.

The neat PCL sample showed a tensile strength of 6.5MPa. The increase in strength was very small at low concentrations of HAP (0.5 wt %), whereby the addition of 1 wt % of HAP resulted in a 12% increase in strength compared to the neat PCL sample. With the addition of 2 wt % HAP, the strength increased by 29%. Hydroxylapatite strongly enhances mechanical performance and hardens the PCL scaffold through the particle dispersion inside the polymer matrix. As the HAP concentration is increased, the mechanical property of the scaffold significantly increased. This is because of the stiffer mechanical properties of HAP in the composite material. This effect is prominent when the amount of HAP does not exceed the value of 2wt %, where there is homogeneous distribution of HAP particle with in the PCL matrix. However with further increase in the HAP concentration, the tensile properties started to deteriorate. At 4wt% HAP concentration, the strength decreased to 6.1MPa. An unexpected drop of the mechanical properties is observed for the high HAP volume fraction i.e., at 6 wt%. This is because of non-homogeneous distribution of HAP. From the above observations, the concentration of HAP to be incorporated in neat PCL system was optimized as 2wt%. [Lee et al., 2010]

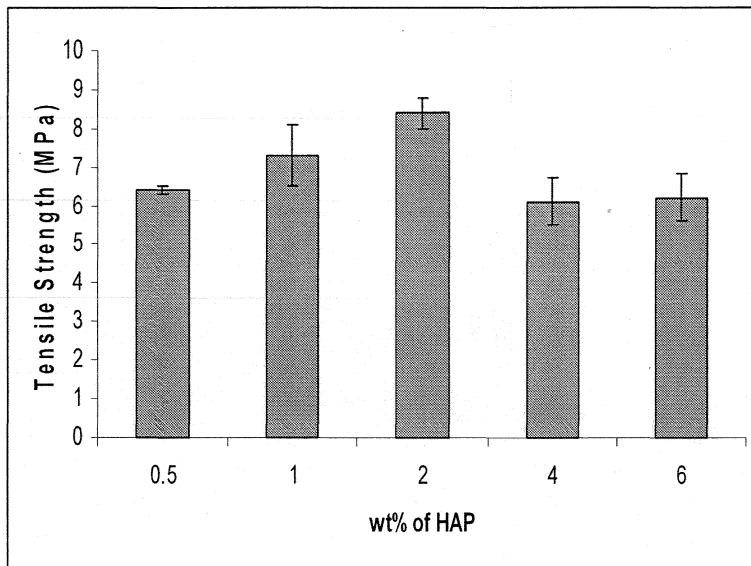


Fig 3.9 Effect of filler content on mechanical strength

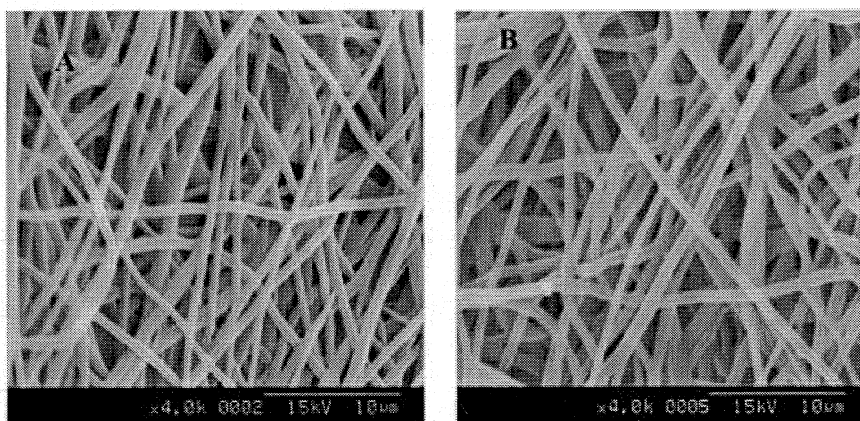
HAP concentration (%)	Fiber diameter (μm)	Tensile strength (MPa)
0.5	0.66 ± 0.13	6.36 ± 0.13
1	0.73 ± 0.14	7.32 ± 0.78
2	0.79 ± 0.15	8.37 ± 0.36
4	0.96 ± 0.26	6.13 ± 0.64
6	0.87 ± 0.16	6.20 ± 0.59

Table 3.2 Effect of filler content on fiber diameter and tensile strength

The quantitative analysis of the fiber diameter from SEM images (fig 3.10) demonstrated that the diameter of PCL/HAP composite nanofiber was in a range of 660-

870 nm. The SEM observation suggests that the roughness of nanofibers was affected by HAP incorporation. Nano HAP had little effect on the nanofibrous morphology at low concentration (0.5 wt %). However, at higher nano HA concentration (6 wt %), a non-uniformity in fiber morphology as well as HAP agglomeration was observed. (Fig 3.10 e)

The addition of nano-HA in the polymer matrix resulted in a slight increase in fiber diameter. This is because presence of non interactive rigid particles increased the shear viscosity of dilute suspensions over that of the neat liquid. The conductivity also decreases for nano composite incorporated polymer solution than that of neat polymer solution. As the viscosity increases and conductivity decreases the fiber diameter increases. [Causa et al., 2005]



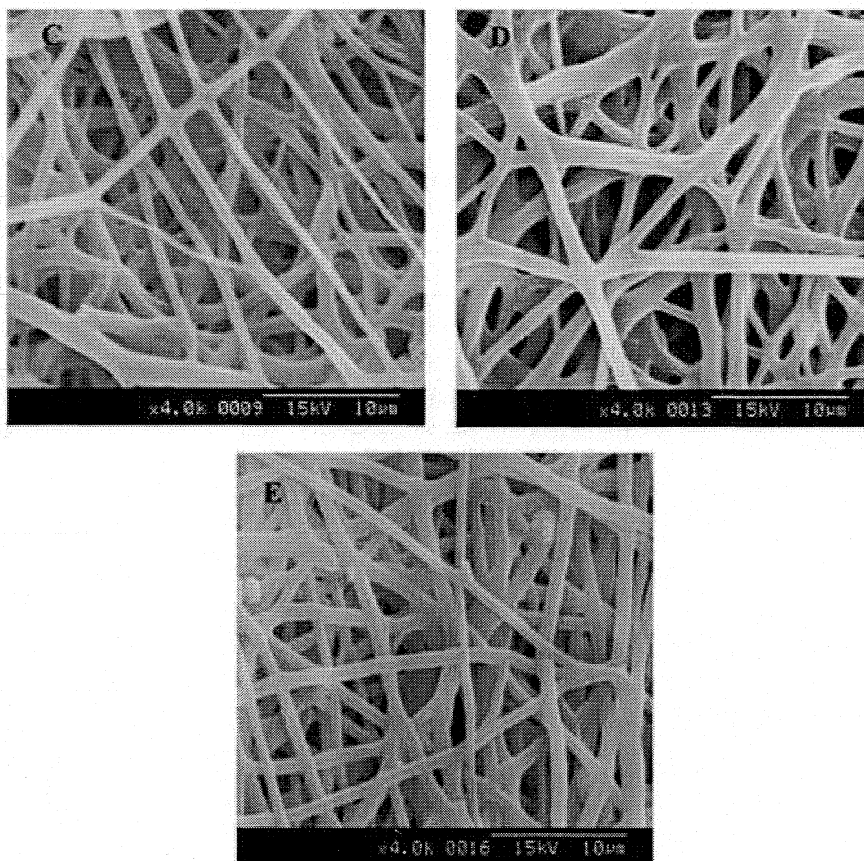


Fig 3.10: SEM micrographs of the electrospun PCL samples at different HAP concentrations; (A) 0.5 wt%, (B) 1 wt%, (C) 2 wt%, (D) 4 wt % and (E) 6 wt%

3.7.3 Effect of triblock copolymer ECE

The tri block copolymer ECE consists of two hydrophilic polyethylene glycol groups with hydrophobic PCL block at the central position. It is expected that scaffolds from electrospun PCL/ECE will be hydrophilic compared to neat PCL. By varying the ratio of PCL and ECE we can easily tune the hydrophilic nature, fiber diameter, and mechanical stability of electrospun fiber. The effect of ECE on neat PCL was evaluated based on mechanical and morphological properties. The variation in mechanical strength and fiber diameter is summarized in Table 3.3. The SEM images of different ratios of copolymer incorporated electrospun scaffold are shown in fig 3.11

Sample PCL/ECE	Fiber diameter μm	Tensile strength (MPa)
90:10	0.75 ± 0.32	$7.86 \pm .72$
80:20	0.73 ± 0.26	7.58 ± 1.69
70:30	0.77 ± 0.22	$6.22 \pm .36$

Table 3.3 Effect of copolymer concentration in fiber diameter and tensile strength

From the above results, considering the hydrophilic as well as mechanical property PCL/ECE ratio was optimized as 90:10

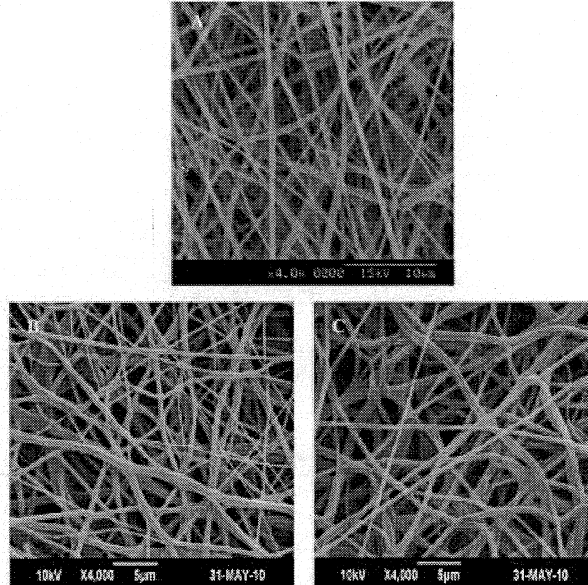


Fig 3.11: SEM micrographs of the electrospun PCL/ECE at different copolymer ratio (A) 90:10 (B) 80:20 (C) 70:30

A novel electrospun fibroporous composite scaffold was fabricated with the optimized conditions using PCL/ECE blend filled with HAP. The effect of various

spinning parameters such as applied potential, feed rate and solvent ratio on morphological and mechanical properties of the composite scaffold was also evaluated.

3.7.4 Effect of Applied Potential

Applied electric field is one of the most important parameters in the electrospinning process. In this process; the electrostatic force in the solutions overcomes their surface tension. The effect of applied potential on the morphological appearance and size of the electrospun fibers was investigated. A mixture of 10%(w/v) PCL and 2 wt% of HA was electrospun under an applied potentials of 12, 15, 17 and 20 kV over a collection distance and mandrel speed of 15cm at 500 rpm respectively.

Table 3.4 shows that variation in average fiber diameter with the increase in electric potential. The analysis showed that with increase in electric potential from 12-17 kV the average fiber diameter decreases from 0.86 to 0.51 μm . Average fiber diameter decreases with the increase in the applied potential from 12kV-17kV. The decrease in diameter with further increase in electrical potential could be due to the dominant effect of the coulombic repulsive force which increases due to the stretching force exerting on the jet segment. As the voltage increases, the charge density within the solution increases leading to higher elongation of the fibers. This in turn reduces the fiber diameter from 860 to 510 nm. [wutticharoenmonkol et al.,2005]

Applied potential	Fiber diameter, μm
12 kV	0.86 ± 0.27
15 kV	0.54 ± 0.09
17 kV	0.51 ± 0.11
20 kV	0.67 ± 0.15

Table 3.4 Effect of applied voltage on fiber diameter

In Contradiction to the above results further increase of applied voltage from 17-20 kV there is an increase in fiber diameter. At 17 kV the fibers get longer flight time than that of 20 kV. It will allow more time for the fibers to stretch and elongate before they are deposited to the collector plate. Thus, at 17kV reduced acceleration of the jet and weaker electric field may favor the formation of finer fibers. But at 20 kV greater amount of charges will cause jet to accelerate faster, and more volume of the solution will be drawn from the tip of needle. [Sarabijith et al 2009]. In fig 3.12 the SEM images of fibers at different voltages are shown.

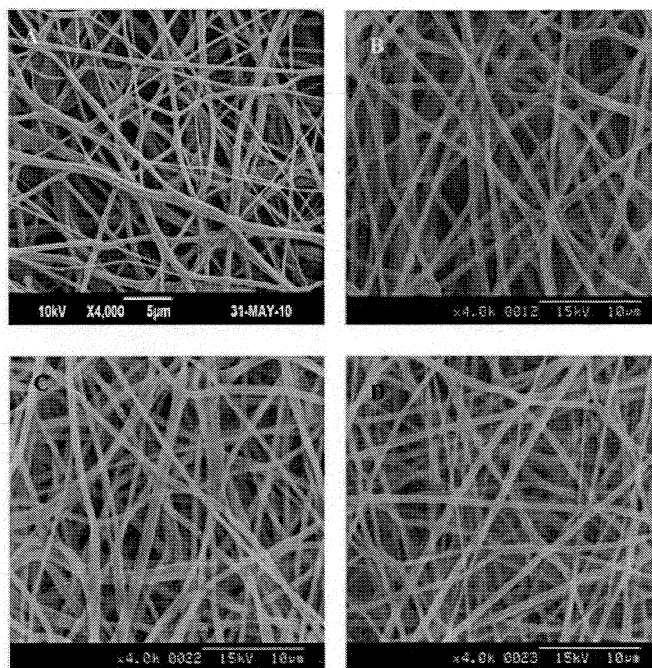


Fig 3.12: SEM micrographs of the electrospun PCL/ECE/HAP samples at different applied potentials; (A) 12kv, (B) 15kv, (C) 17kv, and (D) 20kv.

3.7.5 Effect of Flow Rate

Fig 3.13 shows PCL/ECE/HAP electrospun fibers at different flow rates (0.5ml/h, 1ml/h, 2ml/h, 3ml/h and 4ml/h). All other parameters (solution concentration 10%, HA concentration 2%, effective potential 12 kV, collector distance 15 cm, mandrel rotation 500 rpm) were kept constant. The average fiber diameter decreases by 32% with increase in flow rate from 0.5ml/h to 1ml/h. This is because corresponding increase in charge when feed rate is increased. Thus there is a corresponding increase in the stretching of the solution which counters the increased diameter due to increased volume. the fiber diameter variation is shown in the table 3.5 [Sarabijith et al 2009]

In contradiction to the above observation the fiber diameter increased with further increase in flow rate from 1ml/hr to 3ml/hr. At higher flow rate the volume of polymer solution at the needle tip is greater higher so the electric field is not sufficient to overcome the surface tension. Thus elongation of fibers does not occur effectively leading to larger fiber diameter.

Flow rate	Fiber diameter, μm
0.5ml/h	0.83 ± 0.22
1ml/h	0.56 ± 0.15
2ml/h	0.60 ± 0.11
3ml/h	0.72 ± 0.20

Table 3.5 Effect of flow rate on fiber diameter

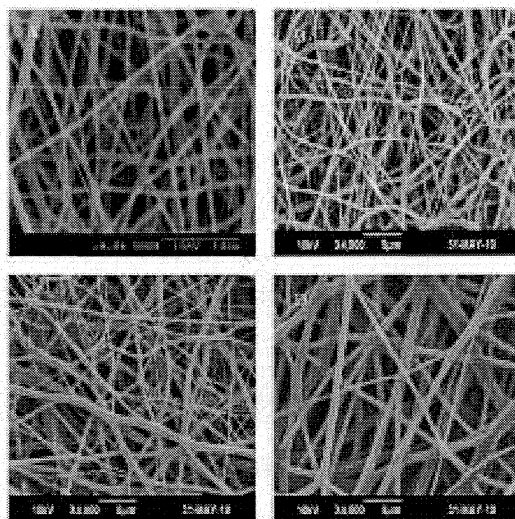


Fig 3.13 SEM micrographs of the electrospun PCL/ECE/HA/P samples at different flow rates: (A) 0.5 ml/hr, (B) 1 ml/hr, (C) 2 ml/hr, (D) 3 ml/hr.

3.7.6 Effect of Solvent ratio

Solvent ratio has an important effect on the fiber diameter and morphology of electrospun polymeric nanofibers. The study is conducted with different solvent ratios of DCM and DMF (90:10, 80:20, 70:30, 60:40, 50:50) by keeping all other parameters constant (10% PCL/ECE/HA solution, 12 kV applied voltage, 15 cm collector distance, 2ml flow rate).

The ratio of DMF added to the solution has a significant effect on the structure of the electrospun polymer. It should be noted that DMF has a boiling point of 153.8°C and is not a solvent for PCL. As a result, the rate of evaporation of liquids (DCM+DMF) from the jet decreases upon the addition of DMF. In this case, the deposition distance can be increased to enhance solvent evaporation. The addition of DMF to the solvent may significantly alter the distribution and size of the fibers obtained on the collector. When DMF ratio increased, the fiber diameter decreases significantly. In addition, a narrow unimodal fiber distribution is observed, compared to the bimodal distribution of fibers produced without any DMF. [Ming Hsu & Shivakumar2003]. Morphology of the obtained fibers are shown in figure 3.14

At a DCM/DMF ratio 90:10 the fiber diameter is 870nm. The thin fibers with narrow fiber distribution were obtained at a DCM/DMF ratio 50:50. In this case average fiber diameter was measured to be 380nm. The reduction in fiber diameter and the change in the fiber distribution with the addition of DMF may be attributed to the extensive splaying that occurs in the jet. DMF enhance the level of jet splaying significantly. When DMF is added to the solution, after the initial elongational flow, the jet almost immediately splits into mini-jets. However, each of these mini-jets splays into a large number of additional very fine mini-jets almost immediately below the needle. It was also observed that the deposition rate and area increase dramatically with DMF addition, as the jet can form, splay and accelerate more easily towards the collector. These results may be explained based on the data of Lee *et al.*, which suggest that DMF additions to the solution may improve electrical conductivity and dielectric constant and lower surface tension. This change in the vital properties associated with jet breakdown may dramatically improve the splitting and splaying processes occurring during the transit of the solution jet to the collector, thereby reducing the fiber diameter appreciably. In particular, Lee *et al.* indicate that the high dielectric constant of DMF may contribute significantly to the reduction in the diameter of the jet. Table 3.6 shows the variation of fiber diameter with different solvent ratios.

Solvent concentration	Fiber diameter, μm
DCM-DMF (5:5)	0.38 \pm 0.10
DCM-DMF (6:4)	0.69 \pm 0.16
DCM-DMF (7:3)	0.71 \pm 0.21
DCM-DMF (8:2)	0.75 \pm 0.32
DCM-DMF (9:1)	0.87 \pm 0.26

Table 3.6 Effect of solvent ratios on fiber diameter

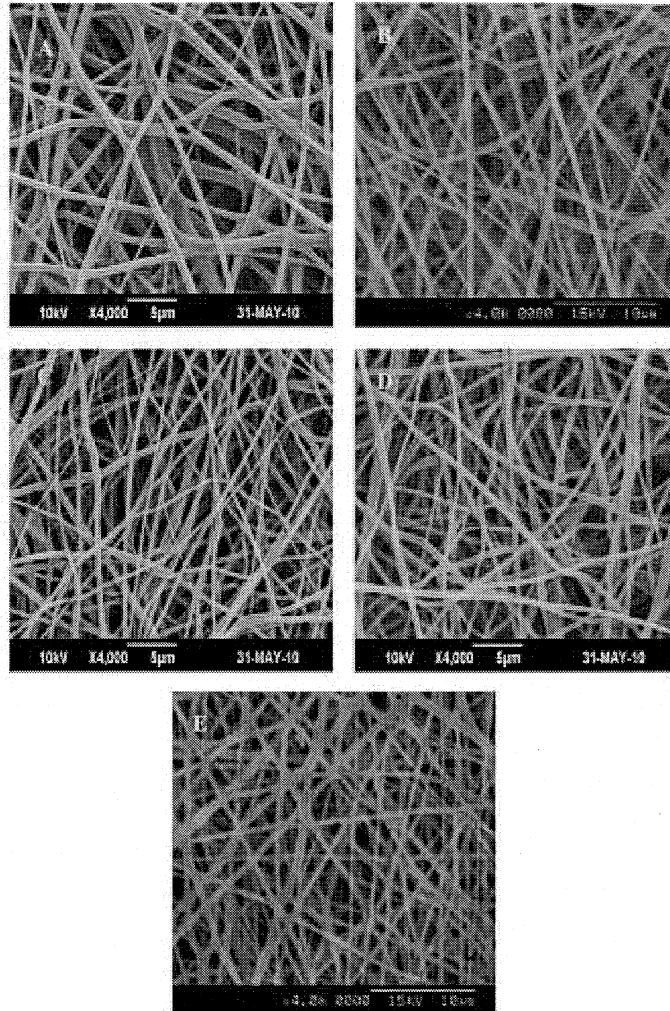


Fig 3.14: SEM micrographs of the electrospun PCL/ECE/HAP samples at different solvent ratios: DCM/DMF (A) 90:10, (B) 80:20, (C) 70:30, (D) 60:40, (E) 50:50

3.8 Comparison of PCL, PCL/HAP, PCL/ECE and PCL/ECE/HAP

Scaffolds using PCL, PCL/ECE blend and there hydroxyapatite filled composites were prepared and analyzed for its static and dynamic mechanical properties, porosity, biostabilty and cytocompatibility. The scaffolds were fabricated under constant

spinning conditions (i.e., 10% solution concentration, 2mL/h feed rate, 12kV applied potential and needle tip to mandrel distance of 15cm) and evaluated. The amount of filler and the polymer - copolymer ratio used were based on the previous studies (i.e. 2wt % HAP and PCL/ECE ratio of 90/10).

3.8.1 Morphological characterization

The SEM images of PCL, PCL/HAP, PCL/ECE, PCL/ECE/HAP are revealed in the fig 3.15 .When the nano HAP filler is added to the neat PCL the conductivity of the solution will decreases and the viscosity of the solution will decreases as a result of this the elongation of fibers during electrospinning will decreases .So the fiber diameter of PCL/HAP is higher than that of neat PCL.

The incorporation of novel hydrophilic tri block copolymer ECE with PCL increases the fiber diameter of electrospun fibers compared to neat PCL as shown in the table 3.7. ECE is a low molecular weight polymer compared to PCL. The higher the molecular weight electrospinnability increases. So the ECE addition decreases the fiber diameter.For PCL/ECE/HAP system the fiber diameter is 0.86 μm

Sample	Fiber diameter
PCL	0.54 \pm 0.17
PCL/HAP	0.85 \pm 0.30
PCL/ECE	0.75 \pm 0.32
PCL/ECE/HAP	0.86 \pm 0.27

Table3.7 Fiber diameter of PCL,PCL/HAP,PCL/ECE,PCL/ECE/HAP scaffolds

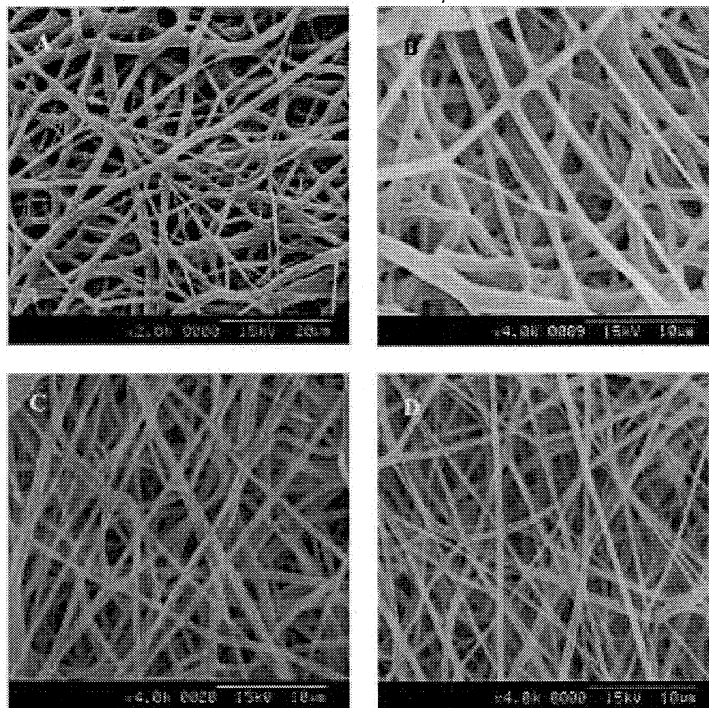


Fig 15: SEM images of (A)PCL,(B) PCL/HAP,(C)PCL/ECE, (D)PCL/ECE/HAP electrospun samples

3.8.2 Mechanical Characterization of scaffolds

The mechanical property of a scaffold is an important aspect. The purpose of the scaffold is not only for providing a surface for cell residence but also for maintaining mechanical stability at the defect site of the host. It must provide sufficient biomechanical support during the process of tissue regeneration and degradation.

3.8.2.1 Universal Testing Machine (UTM)

Mechanical properties were determined using UTM and the results are summarized in the table 3.8. The tensile strength of neat PCL electrospun sample is 6.5MPa. Addition of nano filler HAP increases the tensile strength of electrospun PCL sample by 29%. HAP is a hard brittle ceramic material because of its brittle nature it

increase the tensile strength of electrospun scaffold. ECE also increases the mechanical stability of PCL electrospun scaffold. The interaction between PCL-ECE is greater than PCL-PCL interaction so the mechanical strength become increased. The bar diagram of mechanical strength of the four scaffolds are shown in fig 3.16

Sample	Tensile Strength (MPa)	Elongation at break (%)	Young's Modulus (MPa)
PCL	6.5 ± 0.4	114.5 ± 10.4	21.2 ± 4.1
PCL/HAP	8.4 ± 0.4	182.5 ± 15.7	21.1 ± 2.7
PCL/ECE	7.9 ± 0.7	185.0 ± 44.7	20.9 ± 4.3
PCL/ECE/HAP	8.3 ± 0.3	182.3 ± 21.5	14.1 ± 2.2

Table 3.8 Mechanical properties of scaffolds using UTM

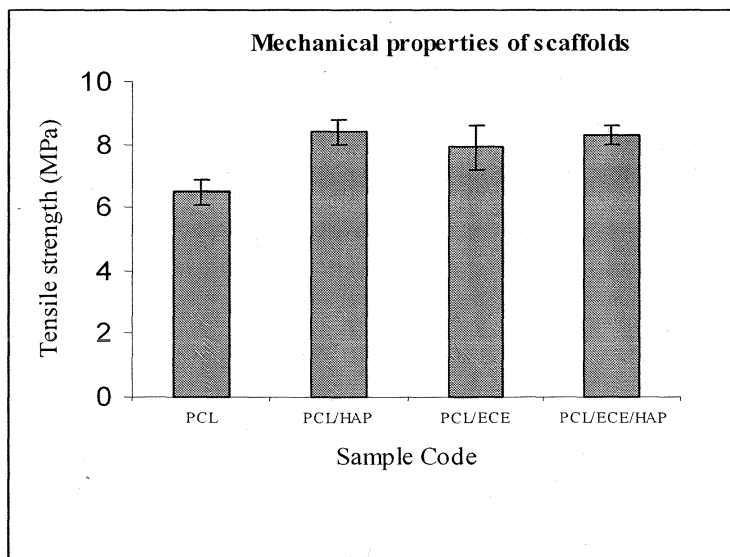


Fig 3.16 Mechanical properties of PCL, PCL/HAP, PCL/ECE, PCL/ECE/HAP electrospun samples

From the observations, it is evident that addition of both ECE and HAP increased the mechanical properties of neat PCL.

3.8.2.2 Dynamic Mechanical Analysis (DMA)

The visco-elastic properties like storage modulus, loss modulus and damping factor ($\tan \delta$) of scaffolds were investigated over a temperature range of $-100\text{ }^{\circ}\text{C}$ to $40\text{ }^{\circ}\text{C}$ under tension mode following the standard technique under the following conditions; a scan rate of $1\text{ }^{\circ}\text{C}/\text{min}$ and a frequency of 1 Hz . The storage modulus and $\tan \delta$ curve of the scaffolds as a function of temperature are shown in figures (fig 3.17 and 3.18)

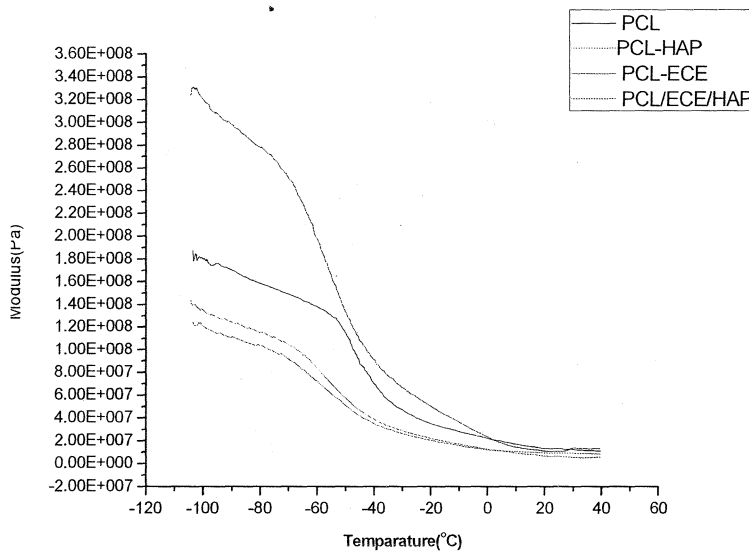


Fig 3.17 Storage modulus of scaffolds as a function of temperature

The storage modulus at 37°C for PCL, PCL/HAP, PCL/ECE and PCL/ECE/HAP were 11.2, 5.3, 13.0 and 8.6 MPa respectively.

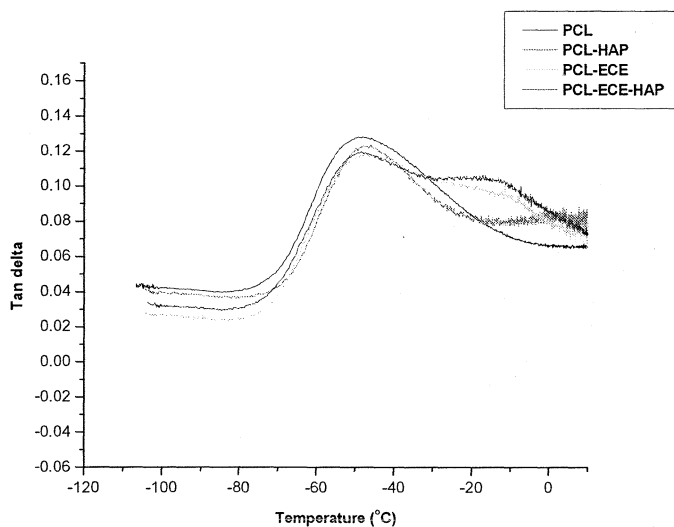


Fig 3.18 Tan delta of scaffolds as a function of temperature

The temperature corresponding to the $\tan \delta$ peak is taken as the glass transition temperature (T_g) of the polymer. The T_g obtained for PCL, PCL/HAP, PCL/ECE and PCL/ECE/HAP were -48.1 , -47.6 , -46.6 and -48.6°C respectively.

3.8.3 Porosity of Scaffolds

Micro-CT is a capable tool which enables the three dimensional characterization of scaffolds. The use of 2D analysis and 3D reconstruction software allows the examination of architecture of as-fabricated scaffolds and provides a quantitative measurement of porosity and pore size distribution. The bar diagram of porosities as well as average pore size of scaffolds measured using micro CT are presented in Fig 3.15.

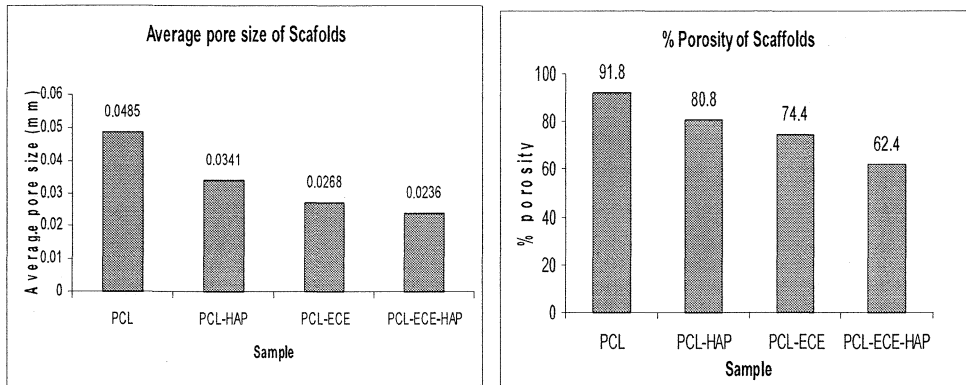
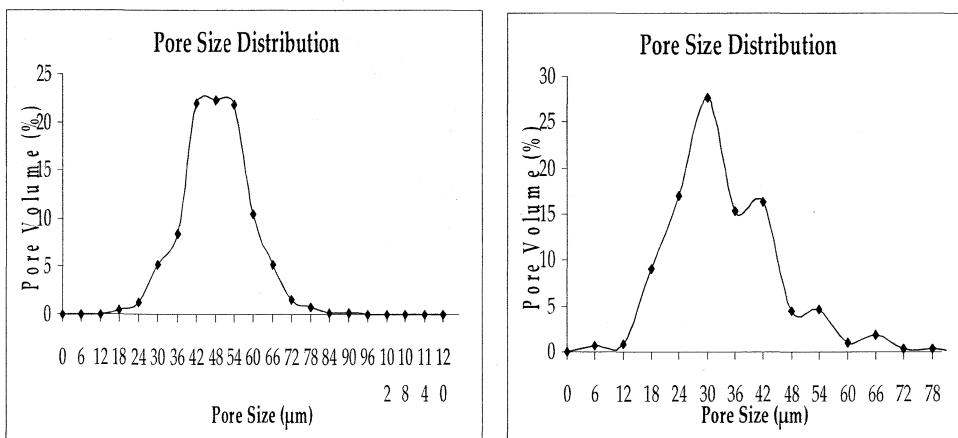


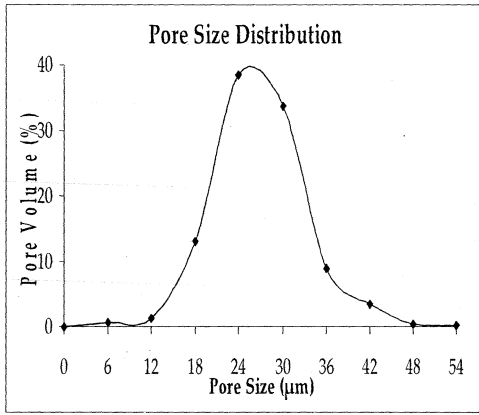
Fig 3.19 Comparative study on the average pore size and % porosity of scaffolds

Neat PCL showed a porosity of about 92%. It is clear from the figure that the porosity of the scaffold decreased to 80% with the addition of HAP and 74 % with that of synthesized copolymer ECE. The fibrous scaffold PCL-ECE-HAP showed a percentage porosity of 62.4%. Hence it is clear that the incorporation of both ECE and HAP caused an overall decrease in porosity. The average pore size also showed a similar trend. For neat PCL, the average pore size was 48 μm where as the addition of both HAP and ECE decreased the pore size to 34 and 26 μm respectively. PCL-ECE-HAP showed an average pore size of 23 μm. The pore size distribution curves and the 3D morphology for the four systems are given in figures 3.20 & 3.21

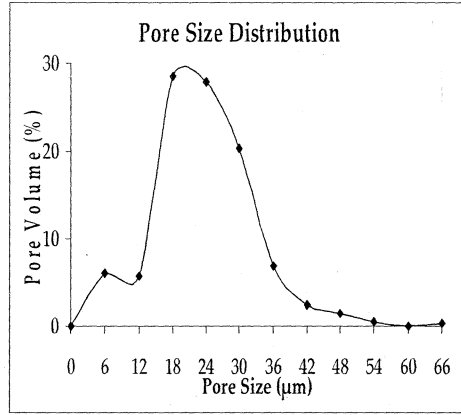


(a)

(b)

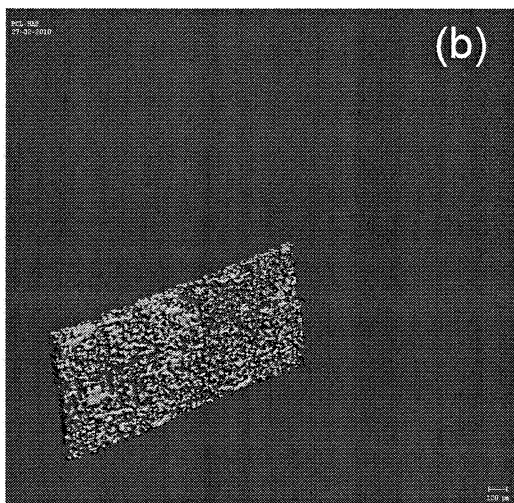
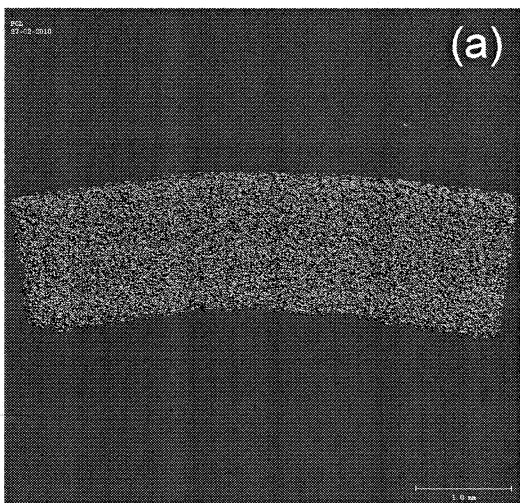


(c)



(d)

Fig 3.20 Pore size distribution curves of (a)PCL,(b)PCL/HAP,(c)PCL/ECE,(d)PCL/ECE/HAP scaffolds



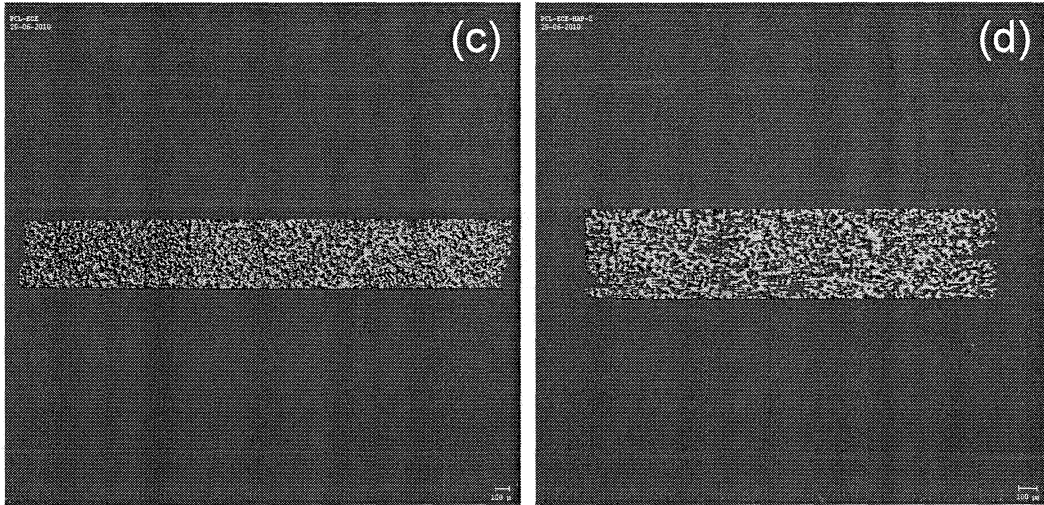


Fig 3.21 Micro-CT 3D morphology images of electrospun scaffolds
 (a)PCL,(b)PCL/HAP,(c)PCL/ECE,(d)PCL/ECE/HAP

3.8.4 *In-vitro* degradation studies of scaffolds in PBS

Degradation properties are of crucial in biomaterial selection and design. This study was designed to investigate *in vitro* degradation of porous composite scaffold for applications in bone tissue engineering. The results obtained for the study of degradation in tensile strength on 0, 2, 7, 14 and 28 days is shown in Fig. 3.22. *In vitro* biodegradation impacted negatively to the mechanical properties of all the four scaffolds, i.e. the tensile strength of the aged electrospun scaffolds decreased with time.

The tensile strength decreased by 42, 55, 28 and 45 % for PCL, PCL-HAP, PCL-ECE and PCL-CEC-HAP respectively by 28 days of PBS aging. The SEM morphology of 28 days degradation samples are in fig 3.23.

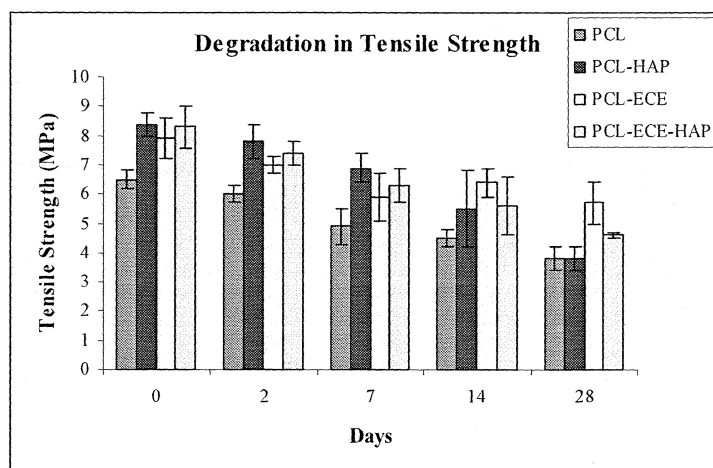


Fig 3.22: Degradation in Tensile Strength of Electrospun samples

The morphology of the samples after 28 days aging in PBS is shown in Fig 3.19

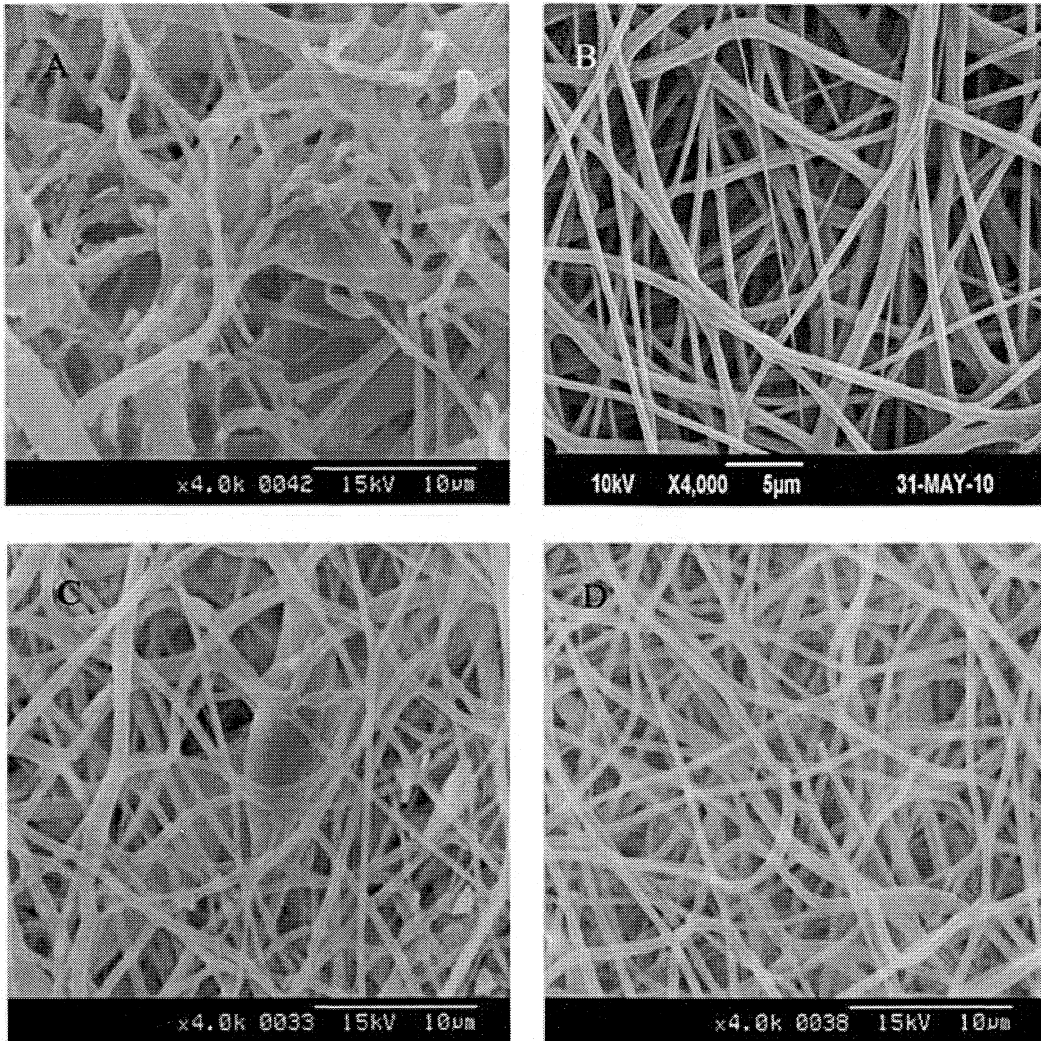


Fig 3.23 SEM images after 28 days aging in PBS
a)PCL,(b)PCL/HAP.(c)PCL/ECE(d)PCL/ECE/HAP

3.8.5 Cytotoxicity evaluation of scaffolds using MTT assay

Apart from favorable physico-chemical and mechanical properties, the most important requirement for a biomaterial to be used in medical application is its biocompatibility in a specific environment, together with the non cytotoxicity of its degradation products. In this study an indirect cytotoxicity test was conducted on fibrous

scaffolds that were prepared from 10% (w/v) PCL solution and from its composites by using L929 cell lines.

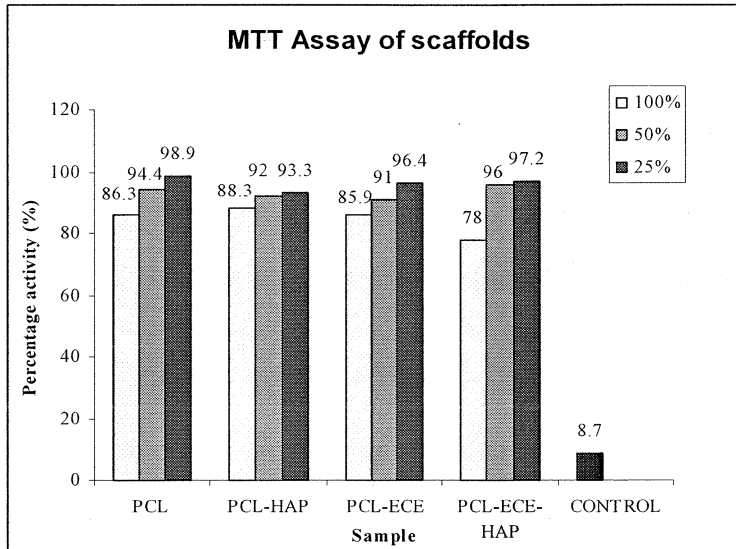


Fig 3.24 MTT assay of the four PCL,PCL/HAP,PCL/ECE,PCL/ECE/HAP scaffolds

Fig 3.24 shows the percentage of metabolic activity obtained from an MTT assay of the cells which were cultured with the extraction media in comparison with those cultured with the control. The MTT Assay of L929 cells after contact with 100%, 50% and 25% extract of test material, PCL alone showed 86.3%, 94.4% and 98.9%, PCL/ECE showed 85.9%, 91% and 96.4%, PCL/HAP 88.3%, 92% and 93.3% and PCL/ECE/HAP 78%, 96% and 97.2% metabolic activity respectively.

Chapter 4

Summary & Conclusions

In the present work, a triblock copolymer consisting of non toxic biocompatible hydrophilic poly (ethylene glycol) and biodegradable hydrophobic polycaprolactone (PCL) of the type PEG-PCL-PEG (ECE) was successfully synthesized. The yield of the prepared copolymer was about 72%. The structural analysis using FTIR and NMR supports the formation of the copolymer. The GPC analysis showed a monomodal molecular weight distribution with PDI of 1.038. The thermo gravimetric analysis indicated that the copolymer is thermally stable up to 201°C.

The synthesized copolymer was further solution blended with PCL. Scaffolds were fabricated using PCL and PCL/ECE blends. Nano hydroxyapatite (HAP) filled PCL and PCL/ECE composite scaffolds were also fabricated. The influence of solution concentration on the morphology of electrospun fibers was initially investigated for PCL. It was revealed from the SEM images that the fibers exhibited a rougher surface morphology with increasing solution concentration. The effect of synthesized copolymer and the filler HAP on mechanical and morphological property of PCL was also evaluated. Mechanical properties depict the non homogenous distribution of HAP particles at loadings beyond 2 wt%. Based on the observations, an optimum solution concentration of 10%, HAP content of 2 wt% and PCL to ECE ratio of 90:10 was chosen. The effect of processing parameters such as applied potential and feed rate on the morphology of the hydroxyapatite filled PCL/ECE blends was investigated. A reduction in fiber diameter was observed with increasing potential (up to 17kV) whereas the fiber diameter increased with increasing feed rate. Minimum fiber diameter was observed with feed rate of 1mL/h. It was also observed that minimum fiber diameter was observed with feed rate 1mL/h and 50:50 solvent ratio (DCM & DMF).

A comparative study of physico-mechanical properties, biostability and cytotoxicity was conducted for PCL, PCL/ECE, PCL/HAP and PCL/ECE/HAP scaffolds.

The tensile strength of neat PCL electrospun sample was 6.5MPa while by the addition of 2wt % of HAP the tensile strength increased by 29%. The introduction of ECE also increased the tensile strength. This increase may be attributed to the better interaction between PCL and the triblock copolymer, ECE. Micro computed tomography analysis revealed a reduction in scaffold porosity from 92 to 80% with the incorporation of nano HAP. The addition of ECE to neat PCL significantly reduced the porosity to about 74 %. PCL-ECE-HAP scaffold showed a percentage porosity of 62%. Hence it is clear that the incorporation of both ECE and HAP caused an overall decrease in porosity. However the pore size is 26 μm which is reported to be sufficient for cell in-growth. As expected the *in vitro* biodegradation decreased the mechanical properties of all the four scaffolds because of the degradation of the matrix. The cytocompatibility evaluation was conducted with mouse fibroblasts cells and all the scaffolds showed non cytotoxic nature. Thus it can be concluded that the composite synthesized herein is a potential material for bone tissue engineering.

Future scope

The fabricated scaffolds have enormous applications in biomedical field especially in bone tissue engineering. The present study confirmed the mechanical and biological compactability of the composite scaffolds but to make these composite scaffolds suitable for such advanced applications further specific tests should be done to evaluate the biological performance like cell attachment and viability studies. Moreover its conformity with the *in vivo* models has to be elucidated by monitoring the short term and long term effects after implantation and later by clinical trials. Apart from bone tissue engineering these composite scaffolds can find various applications in cranioplasty, maxillofacial reconstruction etc.

APPENDIX

Phosphate buffered saline (abbreviated PBS) is a buffer solution commonly used in biological research. It is a salty solution containing sodium chloride, sodium phosphate, and (in some formulations) potassium chloride and potassium phosphate. The buffer helps to maintain a constant pH. The ion concentrations of the solution usually match those of the human body. PBS has many uses because it is isotonic and non-toxic to cells.

For 1 litre of Phosphate-buffered saline (PBS buffer) use:

Dissolve in 800 ml of distilled H₂O:

- 8 g of NaCl
- 0.2 g of KCl
- 1.44 g of Na₂HPO₄ · 12H₂O and
- 0.24 g of KH₂PO₄
- Adjust the pH to 7.4 with HCl
- Add H₂O to 1 liter

REFERENCES

- Athreya SA, Martin DC. Impedance spectroscopy of protein polymer modified silicon micromachined probes. *Sensors and Actuators a—Physical*. 1999; 72(3):203–216.
- Baumgarten PK. Electrostatic spinning of acrylic microfibers. *J of Colloid and Interface Science* 1971;36:71–92.
- Bogdanov B, Vidts A, Bulcke VD, Verbeeck R, Schacht E. Synthesis and thermal properties of poly(ethylene glycol)-poly(ε-caprolactone) copolymers. *Polymer* 1998; 39:1631–6.
- Burdick JA. and Anseth KS. Photo encapsulation of osteoblasts in injectable RGD-modified PEG hydrogels for bone tissue engineering. *Biomaterials* 2002 ;23(22): 4315-4323
- Calandrelli L, Immirzi B, Malinconico M. Natural and synthetic hydroxyapatite filled PCL: mechanical properties and biocompatibility analysis. *Journal of bioactive and compatible polymers*. 2004; 19:301-313.
- Casper CL, Stephens JS, Tassi NG, Chase DB, Rabolt, JF. High-Temperature Electrospinning of Polyethylene Microfibers from Solution Macromolecules 2004;37:573–578.
- Causa F, Netti PA, Ambrosia L, Ciapetti G, Baldini N, Pagani S, Martini D, giunti A. Poly-ε-caprolactone/hydroxyapatite composites for bone regeneration: in vitro characterization and human osteoblast response. *J. Biomedical Material Research*. 2006; 76:151-162.
- Chew SY , Wen Y, Dzenis Y, Leong KW .The Role of Electrospinning in the Emerging Field of Nanomedicine. *Curr Pharm Des*. 2006; 12(36): 4751–4770.

- Christopher X, Lam F, Dietmar I, Hutmacher W, Schantz JT, Woodruff MA, Teoh Sh. Evaluation of polycaprolactone scaffold degradation for 6 months in vitro and in vivo. *Journal of Biomedical Materials Research Part A* 2009;90(3):906-919.
- Cuong NV, Chen CH, Chen YT, Hsieh MF. Preparation of nanoparticle of methoxy poly(ethylene glycol)/ poly(ϵ -caprolactone)/methoxy poly(ethylene glycol) triblock copolymer for drug delivery applications. *IFMBE Proceedings*. 2008; 19:190-193
- Deitzel JM, Kleinmeyer J, Harris D, Tan NCB. The effect of processing variables on the morphology of electrospun nanofibers and textiles. *Polymer*. 2001; 42: 261-272
- Demir MM, Yilgor I, Yilgor E, Erman B. Electrospinning of polyurethane fibers. *Polymer* 2002; 43:3303–3309.
- Ding B, Kimura E, Sato T, Fujita S, Shiratori S. Fabrication of blend biodegradable nanofibrous non woven mats via multi-jet electrospinning. *Polymer* 2004; 45: 1895-1902.
- Doshi J, Reneker DH. Electrospinning process and applications of electrospun fibers. *J Electrostatics* 1995; 35:151-60.
- Fong H, Chun I, Reneker DH. Beaded nanofibers formed during electrospinning. *Polymer*. 1999; 40: 4585- 4592
- Fong H, Reneker DH. Elastomeric nanofibers of styrene-butadiene- styrene triblock copolymer. *J Polym Sci: Part B Polym Phys*. 1999;37(24):3488–93.
- Fujihara K, Kotaki M, Ramakrishna S. Guided bone regeneration membrane made of polycaprolactone/calcium carbonate composite nano-fibers. *Biomaterials*. 2005; 26(19): 4139—4147

- Gupta P, Elkins, Long TE, Wilkes GL. Electrospinning of linear homopolymers of poly(methyl methacrylate): exploring relationships between fiber formation, viscosity, molecular weight and concentration in a good solvent. *Polymer* 2005; 46: 4799-4810
- Hsu CM and Shivkumar S. Nano-sized beads and porous fiber constructs of Poly(ϵ -caprolactone) produced by electrospinning. *Journal of Materials Science*. 2004; 39: 3003 – 3013.
- Hsu CM and Shivkumar S. N,N – Dimethylformamide addition to the solution of the electrospinning of Poly(ϵ -caprolactone) nanofibres. *Macromolecular materials and engineering*. 2004;289:334-340.
- Hutmacher DW. Scaffolds in tissue engineering bone and cartilage. *Biomaterials*. 2000;21: 2529-2543.
- Ignatious F, Baldoni JM. Electrospun pharma-ceutical compositions, WO Pat. 2001;(1)546-567.
- Inai R, Kotaki M, Ramakrishna S. Deformation behavior of electrospun P(LLA-CL) nonwoven membranes under uniaxial tensile loading. *Polymer Sci* 2004. submitted for publication
- Jaeger R, Bergshoef MM, Battle CMI, Schonherr H, Vancso GJ. Electrospinning of ultra-thin polymer fibers. *Macromol Symp* 1998 ;127:141-50.
- Jiang HL, Fang DF, Hsiao BS, Chu B, Chen WL. Optimization and characterization of dextran membranes prepared by electrospinning. *Biomacromolecules* 2004; 5:326-333
- Jose MV, Thomas V, Xu Y, Bellis S, Nyairo E, Dean D. Aligned Bioactive Multi-Component Nanofibrous Nanocomposite Scaffolds for Bone Tissue Engineering, *Macromol. Biosci* 2010; 10:433–444

- Kikuchi M, Suetsugu Y, Tanaka J, Akao M. Preparation and mechanical properties of calcium phosphate/copoly-L-lactide composites. *J Mater Sci Mater Med* 1997; 8:361–364.
- Kim HS, Kim K, Jin HJ, Chin IJ. Morphological characterization of electrospun nanofibrous membranes of biodegradable poly(L-lactide) and poly(lactide-co-glycolide). *Macromol. Symp.* 2005; 145:224-229.
- Kweona H, Yoob MK, KyuPark I, Kimb TH, Leec HC, Leec HS, Ohc JS, Akaiked T, Chong-SuCho b. A novel degradable polycaprolactone networks for tissue engineering. *Biomaterials.* 2003; 24 :801–808
- Lee JS, Choi KH, Do Ghim H, Kim S., Chun DH, Kim HY, Lyoo, W.S. Role of molecular weight of atactic poly(vinyl alcohol) (PVA) in the structure and properties of PVA nanofabric prepared by electrospinning. *J. Appl. Polym. Sci.* 2004; 93: 1638- 1646.
- Lee K, Kim H, Bang H, Jung Y, Lee S. *Polymer.* 2003;44:4029.
- Li XH, Zhang YH, Yuan RH, Deng XM. Influence of process parameters on the protein stability encapsulated in poly dl-lactide-poly(ethylene glycol)microspheres. *J Control Release* 2000; 68: 41–52.
- Liu HQ and Hsieh YL. Ultrafine fibrous cellulose membranes from electrospinning of cellulose acetate. *J. Polym. Sci. B-Polym. Phys.* 2002; 40: 2119-2129
- Liu Q, de Wijn JR, Bakker D, Van Blitterswijk CA. Surface modification of hydroxyapatite to introduce interfacial bonding with polyactive™ 30/70 in a biodegradable composite. *J Mater Sci Mater Med* 1996; 7:551–557.
- Lu C, Guo S, Zhang Y, Yin M. Synthesis and aggregation behavior of four types of different shaped PCL-PEG block copolymers. *Polym Int.* 2006; 55:694–700
- Marra KG, Szem JW, Kumta PN, DiMilla PA, Weiss LE. In vitro analysis of biodegradable polymer blend/hydroxyapatite composites for bone tissue engineering. *J Biomed Mater Res* 1999; 47:324–35.

- Mattanavee W, Suwantong O, Puthong S, Bunaprasert T, Hoven VP, Supaphol P. Immobilization of Biomolecules on the Surface of Electrospun Polycaprolactone Fibrous Scaffolds for Tissue Engineering, *Appl. Mater. Interface*. 2009; 1 (5):1076–1085
- Meechaisue C, Dubin R, Pitt S, Hoven VP, Kohn J. Electrospun Mat Of Tyrosine-Derived Polycarbonate Fibers for potential use as tissue scaffolding material. *J. Biomater. Sci. Polymer* 2006; 17(9):1039–1056
- Megelski S, Stephens JS, Chase DB, Rabolt JF. Micro- and nanostructured surface morphology on electrospun polymer fibers. *Macromolecules* 2002; 35(22):8456-8466.
- Mit-Uppatham C, Nithitanakul M, Supaphol P. Ultrafine electrospun polyamide-6 fibers: effect of solution conditions on morphology and average fiber diameter. *Macromol. Chem. Phys.* 2004; 205: 2327-2338
- Murugan R, Ramakrishna S. Design Strategies of Tissue Engineering Scaffolds with Controlled Fiber Orientation. *Tissue Engineering* 2007; 13(8): 1845-1866.
- Nie T, Zhao Y, Xie Z, Wu C. Micellar Formation of Poly(caprolactone-block-ethylene oxide-block- caprolactone) and Its Enzymatic Biodegradation in Aqueous Dispersion. *Macromolecules* 2003; 36:8825-8829.
- Pham QP, Sharma U, Mikos AG. Electrospun Poly(ϵ caprolactone) Microfiber and Multilayer Nanofiber/Microfiber Scaffolds: Characterization of Scaffolds and Measurement of Cellular Infiltration. *Biomacromolecules* 2006; 7 (10):2796–2805
- Ratner BD. Biomaterial science; An interdisciplinary endeavour. In. Ratner BD, Hoffman AS, Schoen FJ, Lemons JE .*Biomaterial science: An introduction to materials in medicine*. London: Academic Press; 1996:1-8
- Ryan R, Duling, Dupaxl RB. Mechanical Characterization of Electrospun Polycaprolactone(PCL): A Potential Scaffold for Tissue Engineering. *Journal of Biomechanical Engineering* . 2008; 130 :1-13.

- Mattanavee W, Suwantong O, Puthong S, Bunaprasert T, Hoven VP, Supaphol P. Immobilization of Biomolecules on the Surface of Electrospun Polycaprolactone Fibrous Scaffolds for Tissue Engineering, *Appl. Mater. Interface*. 2009; 1 (5):1076–1085
- Meechaisue C, Dubin R, Pitt S, Hoven VP, Kohn J. Electrospun Mat Of Tyrosine-Derived Polycarbonate Fibers for potential use as tissue scaffolding material. *J. Biomater. Sci. Polymer* 2006; 17(9):1039–1056
- Megelski S, Stephens JS, Chase DB, Rabolt JF. Micro- and nanostructured surface morphology on electrospun polymer fibers. *Macromolecules* 2002; 35(22):8456-8466.
- Mit-Uppatham C, Nithitanakul M, Supaphol P. Ultrafine electrospun polyamide-6 fibers: effect of solution conditions on morphology and average fiber diameter. *Macromol. Chem. Phys.* 2004; 205: 2327-2338
- Murugan R, Ramakrishna S. Design Strategies of Tissue Engineering Scaffolds with Controlled Fiber Orientation. *Tissue Engineering* 2007; 13(8): 1845-1866.
- Nie T, Zhao Y, Xie Z, Wu C. Micellar Formation of Poly(caprolactone-block-ethylene oxide-block- caprolactone) and Its Enzymatic Biodegradation in Aqueous Dispersion. *Macromolecules* 2003; 36:8825-8829.
- Pham QP, Sharma U, Mikos AG. Electrospun Poly(ϵ caprolactone) Microfiber and Multilayer Nanofiber/Microfiber Scaffolds: Characterization of Scaffolds and Measurement of Cellular Infiltration. *Biomacromolecules* 2006; 7 (10):2796–2805
- Ratner BD. Biomaterial science; An interdisciplinary endeavour. In. Ratner BD, Hoffman AS, Schoen FJ, Lemons JE .*Biomaterial science: An introduction to materials in medicine*. London: Academic Press; 1996:1-8
- Ryan R, Duling, Dupaxl RB. Mechanical Characterization of Electrospun Polycaprolactone(PCL): A Potential Scaffold for Tissue Engineering. *Journal of Biomechanical Engineering* . 2008; 130 :1-13.

- Sill TJ, von Recum HA. Electrospinning: applications in drug delivery and tissue engineering. *Biomaterials*. 2008; 29(13):1989-2006.
- Singh S, Lakshmi SG, Vijayakumar M. Effect of process parameters on the microstructural characteristics of electrospun poly(Vinyl Alcohol) fiber mats. *Nanobiotechnol*. 2009; 5: 10-16.
- Sui G, Yang X, Mei F, Hu X, Chen G, Deng X, Seungkon. Poly-L-lactic acid/hydroxyapatite hybrid membrane for bone tissue regeneration, *J Biomed Mater Res A*. 2007; 82(2):445-54.
- Tuzlakoglu K, Bolgen N, Salgado AJ et al. Nano- and micro-fiber combined scaffolds: A new architecture for bone tissue engineering. *J Mater Sci: Mater Med*, 2005, 16(12): 1099—1104
- Venugopal JR, Zhang Y, Ramakrishna S. In Vitro Culture of Human Dermal Fibroblasts on Electrospun Polycaprolactone Collagen Nanofibrous Membrane. *Artif Organs* .2006; 30(6),440-446.
- Webster TJ, Siegel RW, Bizios R. Osteoblast adhesion on nanophase ceramics. *Biomaterials* 1999; 20:1221–1227.
- Wutticharoenmongkol P, Sanchavanakit N, Pavasant P et al. Preparation and characterization of novel bone scaffolds based on electrospun polycaprolactone fibers filled with nanoparticles. *Macromolecul Biosci*. 2006; 6(1): 70—77
- Yoshimoto H, Shin YM, Terai H et al. A biodegradable nanofiber scaffold by electrospinning and its potential for bone tissue engineering. *Biomaterials*. 2003; 24(12): 2077—2082.
- Zhang Y, Ouyang H, Lim CT et al. Electrospinning of gelatin fibers and gelatin/PCL composite fibrous scaffolds. *J Biomed Mater Res Part B: Appl Biomater*. 2005;72(1): 156—165.

- Zheng-Ming Huang , Chuang-Long He , Aizhao Yang , Yanzhong Zhang , Xiao-Jian Han , Junlin Yin , Qingsheng Wu . Encapsulating drugs in biodegradable ultrafine fibers through co-axial electrospinning. *Journal of Biomedical Materials Research Part A* 2006 ;77(1):169 – 179.
- Zong XH., Kim K., Fang DF, Ran SF, Hsiao BS, Chu B. Structure and process relationship of electrospun bioabsorbable nanofiber membranes. *Polymer*. 2002; 43(16): 4403-4412
- Zuo WW, Zhu MF, Yang W, Yu H, Chen YM, Zhang Y. Experimental study on relationship between jet instability and formation of beaded fibers during electrospinning. *Polym. Eng. Sci.* 2005; 45: 704-709